University of Stavanger

RAVN L. ENGAMO & PETTER TAJET
SUPERVISOR: SUDATH C. SIRIWARDANE

Load Capacity of a Steel Bridge

Effect of Corrosion for Lateral-Torsional Buckling Capacity

Bachelor thesis spring 2024

Konstruksjonsteknikk

Institutt for maskin, bygg og materialteknologi

Det teknisk-naturvitenskaplige fakultet

FACULTY OF SCIENCE AND TECHNOLOGY

BACHELOR'S THESIS

Study programme / specialization: Byggingeniør: Konstruksjonsteknikk	Spring semester 2024 Open/~~Confidential~~
Author: Petter Tajet and Ravn L. Engamo	
Faculty supervisor: Professor Sudath C. Siriwardane	
Thesis title: Load capacity of a steel bridge: Effect of corrosion for lateral-torsional buckling capacity	
Credits (ECTS): 20	
Keywords: Road bridge Corrosion Lateral torsional buckling Structural degradation	Pages: 49 + appendix: 50 Stavanger, 15.05.2024

Acknowledgement

This bachelor`s thesis is the final project for our bachelor's degree in structural engineering, at the Department of Mechanical and Structural Engineering and Materials Science, here in Norway at the University of Stavanger.

Firstly, we would like to express our gratitude to Professor Sudath C. Siriwardane of The University of Stavanger for his great support and advice throughout the thesis. His dedication and passion for the subject is truly inspiring, and we are very grateful for his guidance. Additionally, Mr. Siriwardane`s dissertations and lectures has been very helpful throughout the thesis.

Throughout the past three years, The University of Stavanger has provided us with valuable knowledge in structural analysis. However, prior to the thesis, our understanding of corrosion was limited. Over the past months, we have gained a broader understanding exploring topics such as abnormal cross-section behavior, and the effect of corrosion.

We are grateful for the support and resources provided by the Department of Mechanical and Structural Engineering and Materials Science at The University of Stavanger.

Abstract

Bridge authorities worldwide are increasingly aware of the urgent need to address the challenges posed by aging infrastructure, especially as many bridges reach the end of their expected lifespan. Steel bridges are particularly concerning due to their susceptibility to corrosion. Recent bridge failures have emphasized the crucial importance of thoroughly examining bridge durability and structural strength. Considering the persistence forces of nature, it is vital to delve into the complex relationship between corrosion and the mechanical behavior of bridges, with a specific focus on deflection and susceptibility to bending induced lateral-torsional buckling. Corrosion is known to alter key structural properties such as cross-sectional area, moment of inertia, bending capacity, and torsional resistance of steel beams. These changes not only compromise the bridge's structural integrity but also increase the risk of catastrophic failure. Therefore, a detailed understanding of how corrosion affects structural behavior is essential for developing effective strategies to mitigate the negative impacts of aging infrastructure. By understanding the mechanisms through which corrosion affects performance, engineers and policymakers can implement targeted measures to extend their lifespan and ensure safety and reliability of vital transportation networks.

The main findings in the thesis are a proposed wastage model for predicting future corrosion and assess structural integrity. Further, a comparison of three cases is showcased, to understand the behavior of LTB capacity against area loss. Concluding with a noticeable relationship between LTB and area loss due to corrosion.

List of Content

List of Figures

List of tables

List of Symbols

A	Cross-sectional area
I_{y-y}	Moment of Inertia y-y
I_{z-z}	Moment of Inertia z-z
A_{y-y}	Shear area y-y
A_{z-z}	Shear area z-z
I_t	Torsional constant
I_w	Warping constant
M_{cr}	Elastic critical moment for lateral-torsional buckling (LTB)
ϕ_{LT}	Dimensionless resistance factor
h_s	Distance between shear center of each flange
S_y	Section modulus y-y
S_z	Section modulus z-z
$W_{pl,y-y}$	Plastic modulus y-y
$W_{pl,z-z}$	Plastic modulus z-z
K_{y-y}	Radius of gyration y-y
K_{z-z}	Radius of gyration z-z
$M_{c,Rd}$	Design section moment Resistance
$\overline{\lambda}_{LT}$	Non-dimensional slenderness ratio
χ_{LT}	Reduction factor for lateral-torsional buckling (LTB)
$M_{b,Rd}$	Design buckling moment Resistance

List of Abbreviations

LTB	Lateral-torsional buckling
PH	Potential of hydrogen
FEM	Finite Element Method
BIM	Building Information Modelling

1 Introduction

1.1 Background

Bridge authorities are placing considerable emphasis on addressing challenges associated with aging infrastructure, as a majority of bridges worldwide are nearing the end of their intended service life. Replacing all aging bridges is impossible due to high costs associated with decommissioning and construction of new ones. Steel bridges are subjected to repeated traffic loads that may be substantially under their structural resistance limit. Single loads may not result in significant consequences, but continually loads over a period of time may result in structural damage and localized cumulative failure processes known as fatigue.

Together with environmental problems caused by corrosion, it may also cause structural damages to bridges. Especially steel bridges are susceptible to deterioration caused by corrosive environment. Corrosive environment includes various forms such as uniform corrosion, pitting corrosion, crevice corrosion, intergranular corrosion, microbiologically influenced corrosion, and environment-assisted cracking.

Steel bridges are often exposed to harsh environmental conditions and there will over time be a degradation of their coatings and material due to corrosion. Consequently, the thickness of structural steel components will diminish. This reduction will affect various geometric properties that influence the structural behavior, moment of inertia, torsional and warping constants. Corrosion leads to material loss on steel members. This can cause surface roughness, irregularities, corrosion pits, and minimization in cross-sectional characteristics of the members. This reduction in thickness can significantly affect the Lateral torsional buckling (LTB) capacity of plate-girder composite bridges and increase the likelihood of local buckling. But there is a problem about this concept because there are no generalized guidelines available for estimating the remaining LTB capacity of deteriorated or corroded plate girder bridges.

1.2 Research Problem

The structural engineering community has a long history of evolving engineering of structures. With specified guidelines for different structures, with different types of material. As research progress due to factors such as advancement in materials, new discoveries, and sometimes crucial destruction of structures. Therefore, specified guidelines are needed. Historically, there have been instances of bridge collapses. Bridges around the world are nearing the end of their lifespan, and due to this inherent nature of structural degradation due to environmental attack and long-term effect of loadings, failures have

occurred. Primary concerns are fatigue and corrosion in steel bridges. As mechanisms of failures or structural degradation due to mentioned issues are under researched, there are currently no generalized guideline for estimating remaining capacity and/or lifetime of structures. The task is to investigate corrosive impacts on steel, and how this will impact Lateral-Torsional Buckling (LTB) capacity. To investigate this, it is essential to thoroughly understand LTB and properties of the steel structures. Challenges arises when dealing with asymmetrical cross-section. When dealing with a symmetrical cross-section, there is plenty of research and papers on the different properties of a cross-section in different guidelines. Symmetric sections are simple to put straight into calculations, as there is well known research and formulas to use. This makes it easy to follow guidelines and designing different structures. When studying the effect of corrosion wastage on a section, new problems start to occur. Attack of uniform corrosion can result in various combinations of altered cross-sectional dimensions, complicating calculations and necessitating new formulas and approaches to understand their impact on LTB. The thesis aim to figuring out time dependent changes of bending stiffness, torsional stiffness and warping stiffness of the deteriorated cross-section due to uniform corrosion and their effects to reduce LTB capacity of bridge members (i.e.steel beams) with the lifetime.

1.3 Research Objective

1.3.1 General Objective

The objectives of this Batchelor thesis are defined to address concerns regarding deterioration of steel plate-girder bridges, aggravated by corrosive environments. This deterioration poses a significant threat to the safety and functionality of such bridges. The aim of the research is to develop practical solutions for managing aging steel infrastructure, specifically Steel bridges.

Overall, the research objectives are carefully crafted to address immediate concerns of aging infrastructure and provide practical solutions for ensuring the integrity of steel plate-girders in corrosive environments.

1.3.2 Specific Objective

- Develop a comprehensive understanding of degradation mechanisms and corrosion patterns affecting steel plate-girder bridges, with a focus on the Storåna I bridge in Norway as a representative case study.
- Investigate the time-dependent effects of corrosion on key geometric properties of structural steel components, such as effective cross-sectional area, moment of inertia, torsional, and warping constants, considering non-linear relationships inherent in these properties.

- Establish a reliable methodology for estimating the remaining lateral-torsional buckling (LTB) capacity of corroded plate-girder bridges, with a particular emphasis on I-beam bridges, encompassing the intricate interplay between corrosion-induced material loss and structural behavior.
- Develop practical guidelines and recommendations for bridge asset management strategies, to facilitate informed decisions regarding maintenance, repair, and retrofitting interventions aimed at enhancing the structural integrity and durability of corroded steel plate girder bridges.

1.4 Significance

This thesis can contribute to estimating the lifespan of steel bridges and other structures affected by corrosion. Furthermore, the thesis may be beneficial developing methods for calculating asymmetric cross-section properties.

1.5 Scope

Information from a specific bridge (Storåna I bridge) is being utilized to apply a conventional method (Eurocode 3) for determining structural behavior. Additionally, a method proposed by Sudath C. Siriwardane is employed for estimating corrosion.

1.6 Limitations

- Although various corrosion types are explained, only uniform corrosion will be considered in this study.
- Effects from wind, braking forces, or such are not included in this analysis.
- Although the bridge`s cross-section consists of three identical beams, only one will be considered, since no load will be applied.
- The study focuses solely on the structural integrity of the steel beam, as it is the primary structural component of the bridge and the material most affected by corrosive attack.

1.7 Outline of the Thesis

Chapter 1 introduces the study, starting with discussing the background, objective- and problem of the research, followed by the significance, scope and the limitations of the thesis. Chapter 2 discusses theory, introducing corrosion and lateral torsional buckling.

Chapter 3 deals with approaches for assessing the LTB, as well as comprising the different standards of the Eurocode. Furthermore, the software, and the different formulas for assessing the LTB is discussed. Chapter 4, the formulas for predicting the average corrosion penetration and the reduction in cross-sectional area is introduced. Chapter 5 assembles a framework for predicting the LTB

reduction, based on Eurocode and the corrosion wastage model. Chapter 6 covers the specifics of the bridge, in addition to calculating the LTB of three different sections. One section for each case. Chapter 7 calculates the degradation for future buckling-reduction. Chapter 8 compares reduction in area with the reduction in buckling capacity. In addition to this, challenges and concerns are discussed. Chapter 9 highlights the finding, and gives directions for the future, concluding the thesis.

2 Theoretical Background and Literature Review

2.1 Corrosion

2.1.1 Corrosion Introduction

Corrosion is the deterioration of a material, typically a metal (both metallic and non-metallic). This is the result of a chemical reaction with its environment. These reactions occur when metal interacts with substances such as oxygen, water, or acids in the surrounding environment. The most common form of corrosion is rusting, which occurs when steel reacts with oxygen and water to form hydrated iron oxide. Corrosion is a redox reaction, meaning that one ion is oxidized while another is reduced. For corrosion to occur, four conditions must be simultaneously fulfilled. There must be an anode, a cathode, a conduction electrolyte for ionic movement, and an electrical current. If any of these four conditions is absent, corrosion will not occur[1].

Anode: The site where oxidation occurs. The metal corrodes by losing electrons and forming discrete ions in the solution.

$$M \rightarrow M^z + Ze^- \quad (1)$$

M: a metal
Z: the valence of the metal. Z=1,2 or 3 (frequently)
e: electrons

Cathode: The electrode in an electrochemical cell or system where reduction occurs. The site where positive ions gain electrons, leading to a reduction in charge or formation of a new substance. These reactions can form a thin metal layer on the surface, which leads to the gaining of electrons for the oxygen atoms, or production of hydrogen gas.

For pH $\geq$ 7: $2H_2O + O_2 + 4e^- \rightarrow 40H^-$ (2)

For pH $\leq$ 7: $2H^+ + 2e^- \rightarrow H_2$ (3)

For pH = 7 (Neutral): $N^{z+} + ze^- \rightarrow N$ (4)

Electrolyte: Electrolytes are substances that can conduct electricity when it's dissolved in water or another solvent. Electrons travels through the medium of electrolytes when completing this electrochemical circuit.

Electrical connection: For a redox reaction such as corrosion to occur, a connection between the anodic- and cathodic site is vital. A physical connection is needed for the flow of the current when the anode and cathode is not of the same material.

As mentioned, both the anodic- and the cathodic reaction is required for a redox reaction to take place. In the anodic reaction, where oxidation occurs, the iron atoms give away electrons to form iron ions. On the other site, where the cathodic reaction is taking place, oxygen molecules from either the air or water, together with hydrogen ions are combining with electrons lost in the anodic reaction both to remain a neutral charge, but also to form water.

Anodic reaction:

Iron is losing electrons (oxidation)

$$Fe(s) \rightarrow Fe^{2+}(aq) + 2e^{-} \tag{5}$$

(s): Substance is solid state.
(aq): Substance is aqueous, which means that it is dissolved in water.

Cathodic reaction:

Oxygen is gaining electrons (reduction)

$$O_2(g) + 4H^{+}(aq) + 4e^{-} \rightarrow 2H_2O(l) \tag{6}$$

(g): Substance is in a gas state.
(l): Substance is a liquid state.

Combined reaction:

The combined redox reaction, where water and iron ions are formed from the iron reacting with oxygen and water.

$$Fe(s) + O_2(g) + 4H^+(aq) \rightarrow Fe^{2+}(aq) + 2H_20(l) \quad (7)$$

On iron and its alloys such as steel and aluminum, the Fe^{2+}-ions are reacting with the OH^- -ions in the water and will then form iron hydroxide, which later will dry to become rust:

$$Fe_2^+ + 2OH^- \rightarrow Fe(OH)_2 \rightarrow_{drying\ process} \rightarrow Fe_2O_3 \quad (8)$$

Rust is a form of corrosion which appears in a brown-orange color. It can both occur in both dry and wet conditions, however, it appears much faster in humid conditions, due to the water contained in the air. Corrosion can appear in different forms which depends on the different factors; Nature of corrodent, mechanism of corrosion and appearance of the corroded metal:

Nature of corrodent:

The occurrence of corrosion can happen various environmental conditions, wet corrosion requires the presence of moist or liquid, whereas dry corrosion typically needs high-temperature gasses to interact with the metal.

Mechanism of corrosion:

When discussing the mechanism of corrosion, there are two main categories: electrochemical- and direct chemical reactions. Electrochemical reactions consist of the transfer of electrons via an electrolyte, while direct chemical reactions do not involve a transfer of electrons, but rather relies on creating new chemical compounds through direct interaction between the molecules.

Appearance of metal when corroding:

Corrosion either appear uniform or localized. When a metal is undergoing a uniform type of corrosion, the whole surface is corroding at a consistent rate. On the other hand, when corrosion is localized and only affect certain areas, the consequences is often irregularities, pits and sometimes even cracks.

2.1.2 Types of Corrosion

In road bridges, corrosion is quite common due to exposure to humid conditions like rivers, lush valleys, and rainfall, with water frequently seeping downward onto the structure. These factors determine the type of corrosion in road bridges. The most relevant forms are uniform-, pitting-, crevice- and galvanic corrosion.

Uniform corrosion:

In uniform corrosion, corrosive attacks are evenly distributed over either a significant portion of the total area or the entire exposed surface of it[2]. This form of corrosion is relatively easy to manage since the material`s lifespan can be calculated using an immersion test. This test measures the progress of corrosion damage and estimates the reduction in effective cross-sectional properties. When conducting this test, it is important to consider the factor of time when estimating corrosion progression. The general thinning of the surface continues evenly all the way to failure.

Pitting corrosion:

Pitting corrosion is a form of corrosive attack which occurs on the surface's irregularity[3] such as:

- Protective coating has either been poorly applied or damaged.
- The protective oxide film is subjected to localized mechanical- or chemical damage.
- Non-metallic inclusions or other non-uniformities in the metal structure.

Pitting corrosion typically does not affect the global stiffness of structure, but corrosion pits may initiate fatigue and stress corrosion cracking. If the corrosion pit is large enough, it could result in total system failure.

Crevice corrosion:

Crevice corrosion is the most common form of corrosion on steel bridges. It occurs in the contact of either two metal surfaces or one metal- and one non-metal surface[4]. This is particularly common with

bolt, rivets and steel plates used for fastening. Crevice corrosion is often more difficult to detect than other forms of corrosion because it occurs in confined areas and spaces with limited access.

Galvanic corrosion:

Galvanic corrosion is the result of contact between two different metals via an electrolyte[5]. When in contact, the metal with more negative potential initially becomes the anode and starts corroding, while the other metal becomes the cathode and is protected. Seawater is an exceptional electrolyte because it contains a high concentration of sodium chloride (salt), therefore, galvanic corrosion is especially common in marine environments.

2.1.3 Consequences of Corrosive Attacks on Steel Bridges

Causes and effects of corrosion on steel bridges:

When metal is deteriorating, its losing thickness. This is known as corrosion rate and can be estimated by dividing the deterioration over time. Corrosion rate is a crucial factor when estimating lifespan of a steel structure. The rate of corrosion is influenced by concentrations of sulfate-, chloride- and carbonate ions, lower pH-values and levels of stress higher than usual.

The corrosive effect on steel bridges can be studied in the range from catastrophic failures, and all the way down to microscopic detail. According to Kulicki et al. [6], there are four main categories of corrosion effect in steel bridges.

1. **Loss of section**
   The reduction of dimensions in member sections is seen as the most important concern. As dimensions decrease, shear-, axial- and bending capacities will reduce as well. The genuine effect of this depends on where on the member it takes place, as consequences varies on whether the corrosive attack is in the middle, at the end or where the load is located.
2. **Creation of stress raisers**
   Corrosive attacks can lead to formation of holes and notches, which then initiates higher stress concentrations and potentially create cracks in the member.
3. **Introduction of unintentional fixity**

   When corrosive attacks affect moving bridge parts such as hangers and expansion devices, they may become frozen, altering the structure's behavior unexpectedly.

4. **Introduction of unintended movement**

   Pack rust, which is built up corrosion in constricted areas, can generate pressure up to ten thousand psi. A pressure like this can move multiple components of the bridge, and in worst case have damaging effect with catastrophic consequences.

Preventing corrosion

The steel will gradually deteriorate over time, if not maintained properly, this will reduce its dimensions and then properties. The most common type of treatment against corrosion is coating, which is a thin but solid layer applied on the surface of the material, to prevent corrosion-involved elements from combining, which then will prevent the corrosion process from occurring, by creating a barrier. Coating is usually sprayed, welded, or applied using hand tools, all depending on the surface and circumstances.

The research of corrosion prevention is mainly driven by three factors: Economics, safety, and conservation of the environment. When maintaining a bridge, money spent is a crucial factor. To properly maintain a steel structure such as a bridge, is extremely expensive. But as different industries have experienced over the years; poor maintenance of the structure could be even more expensive. In fact, recent studies suggests that if periodic corrosion control is established, the cost of corrosion treatment could be reduced by 25-30% [7]. If the bridge collapses due to improper management of maintenance, the cost will be great, and the maintenance company could be blamed.

Proper treatment of corrosion expansion is necessary to maintain the structures safety. Maintenance is both expensive and time-consuming, as it mostly requires thorough inspection over time. Corrosion does also have an impact on the environment, as it can release waste and substances like iron oxide which causes harm on the environment. When iron oxide is released into the soil or on plants, it can in worst case shut down their growing ability.

2.2 Lateral Torsional Buckling of Beams

2.2.1 Introduction to LTB

The behavior of beams that doesn't have sufficient lateral stiffness or lateral support, may buckle out of the plane due to loading. This type of buckling may occur with substantially lower load than what the beams in-plane load can resist. For a straight elastic I-beam, there will not occur an out-of-plane deformation before there is applied moment *M* from the load, which reaches the elastic buckling moment M_{cr}, and the beam starts deflecting laterally and twisting. These two deformations are dependent to each other. Due to the beam's deflection laterally, the applied moment will have a component which creates a torque about the deflected longitudinal axis which causes the beam to twist. This is also called lateral torsional buckling. Longer beams are more susceptible to lateral torsional buckling. As the length increases, likelihood of buckling under bending loads also increases[8]. Lateral torsional buckling is a critical concern in design of structural members, especially in bridge structures, as they consist of long members.

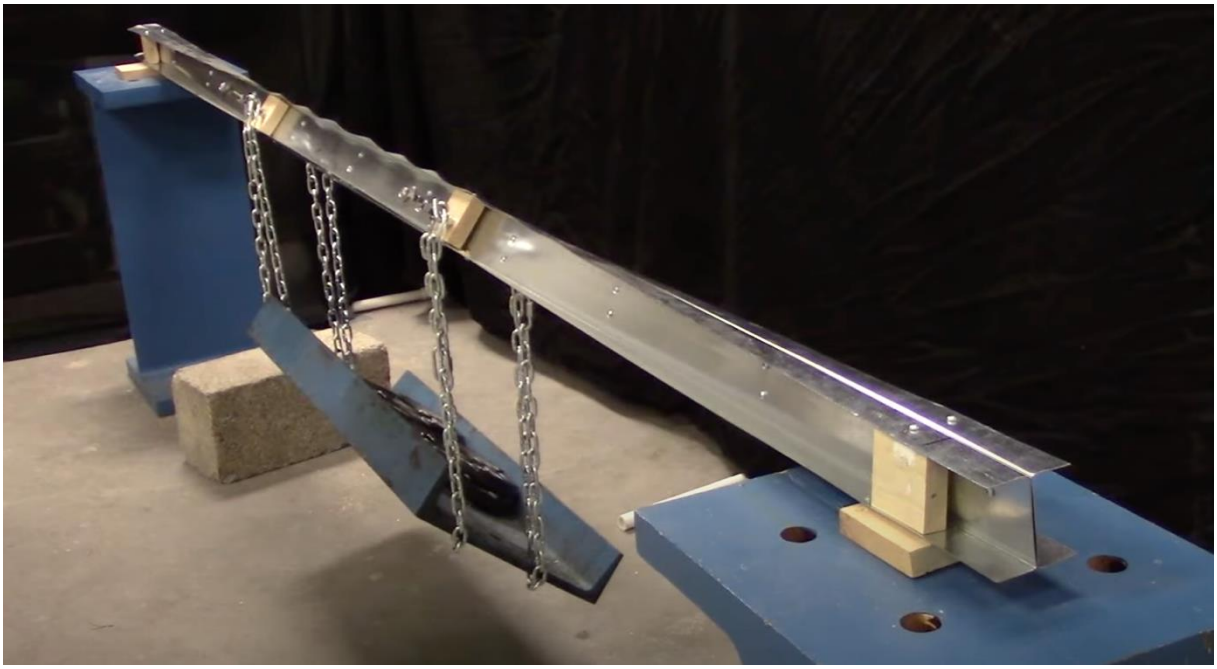

Figure 1: Lateral torsional buckling [9]

2.2.2 LTB Governing Cross-Sectional Properties

To calculate lateral torsional buckling there are formulas that are used to determine if there will occur lateral torsional buckling. Lateral torsional buckling can be affected by the cross-sectional area of the element/beam, moment of inertia, torsional and the warping constant.

Cross-Sectional Area:

The cross-sectional area of an I-beam can be calculated by breaking down the shape into its different geometrical parts and summing up their areas. I-beams typically consists of a central web (the vertical part) and two flanges (the horizontal parts), as shown in Figure 6, the different parts of the I-beam is:

- **b** the width of each flange
- $\mathbf{t_f}$ the thickness of each flange
- **h** the width of the web
- $\mathbf{t_w}$ the thickness of the web
- **r** the radius of the rolled section

Taking this into account, the total cross-sectional area (A) can be calculated as:

$$A_{total} = \Big(\big(b * t_f\big) * 2\Big) + \big(h - 2 * t_f\big) * t_w + (r^2 * (4 - \pi)) \tag{9}$$

Moment of Inertia:

Moment of inertia is a measure of an objects resistance to change in its rotation about a specific axis. It quantifies how the mass of an object is distributed relative to that axis. The moment of inertia determines a beams resistance to bending, and larger moments of inertia lead to greater resistance against lateral-torsional buckling. Complex objects are calculated differently, often involving integration over the objects mass distribution. The moment of inertia can be calculated with the formulas shown under:

$$I_{total} = \sum(\bar{I}_i + A_i * d_i^2) \tag{10}$$

$\boldsymbol{\bar{I}_i = The\ moment\ of\ inertia\ of\ the\ individual\ segment\ about\ its\ own\ centeroid\ axis}$

$\boldsymbol{A_i = The\ area\ of\ the\ individual\ segment}$

$\boldsymbol{d_i = The\ vertical\ distance\ from\ the\ centeroid\ of\ the\ segment\ to\ the\ Neutral\ axis}$

The I-beam is for simplifications divided into three rectangular parts, and each of these sections needs to be calculated. The moment of inertia for a rectangular about its centroid axis is simply:

$$\bar{I} = \frac{1}{12} * b * h^3 \tag{11}$$

$\boldsymbol{b = The\ base/width\ of\ the\ rectangle}$

$\boldsymbol{h = The\ height\ of\ the\ rectangular}$

Simplified: find moment of inertia of each segment then sum them together to get the total moment of inertia.

Torsional and Warping Constant:

Torsional constant (I_t) or torsional coefficient is a geometrical property of a bars cross-section. The torsional constant represents a measure of a beam's resistance to torsion. Mathematically, its defined as the polar moment of inertia of the cross-section about its neutral axis. The torsional constant is crucial in analyzing the torsional deflection and stress distribution in beams subjected to torsional loads. Together with the Warping constant (I_w), there may be an impact on the lateral torsional buckling[10].

The torsional constant is often referred to as $\boldsymbol{I_T}$ or $\boldsymbol{J}$. The torsional constant can be calculated by the two following formulas.

$$I_t = \frac{1}{3} \sum_i b_i t_i^3 \tag{12}$$

$\boldsymbol{b = The\ width\ of\ each\ section}$

$\boldsymbol{t = The\ thickness\ of\ each\ section}$

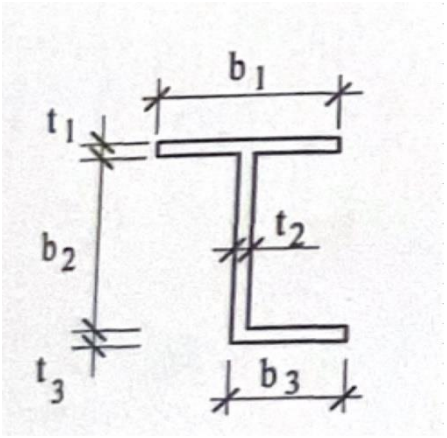

Figure 2: Dimensions for torsional constant

The torsional constant can also be calculated with the following formula:

$$I_t = \frac{2}{3} b\, t_f^3 + \frac{1}{3}(h - 2t_f) t_w^3 + 2 \propto_1 D_1^4 - 0{,}420 t_f^4 \tag{13}$$

Where:

$$\propto = -0{,}042 + 0{,}2204 \frac{t_w}{t_f} + 0{,}1355 \frac{r}{t_f} - 0{,}0865 \frac{r t_w}{t_f^2} - 0{,}0725 \frac{t_w^2}{t_f^2} \tag{14}$$

$$D_1 = \frac{(t_f + r)^2 + (r + 0{,}25 t_w) t_w}{2r + t_f} \tag{15}$$

The warping constant (Iw) is a measure of a beam's resistance to twisting out of plane. The warping constant quantifies a beam's ability to resist warping deformation under torsion. It depends on the beams cross-sectional shape, symmetry, and distribution of material. The following formula shows the warping constant: (It can be calculated in two different ways.)

$$I_w = \frac{1}{24}\, b^3\, h^2\, t \tag{16}$$

$$I_w = \frac{I_z h_s}{4} \tag{17}$$

2.3 Recent Studies on LTB Capacity of Corroded Steel Bridges

The load capacity of corroded steel bridges has gotten more research lately, as this is a big concern for bridge authorities around the world. The research often includes using finite element method (FEM) to determent the flaws of the different steel components of bridges. This is often a good approach, but in some engineering aspects it may be problematic as software doesn't always match reality. On the other hand, it is not easy to do testing of an existing bridge on site. This makes a huge problem with corrosion and its effect on the LTB capacity to investigate.

An article from A. F. Hughes et al. [10] , investigated the uniformed non-uniform corrosion of the bearing stiffener and the web of the I-girder. Their studies included various damage cases. They used FEM for investigating load-carrying capacity of a corroded steel I-girder. During their work they included various corrosion models to calculate the values of shear and bearing capacity. They figured out that the multi-area corrosion patterns, had a significant influence on the load-carrying capacity for the shear or bearing capacity of a steel I-girder end. They also figured out that for their specified corrosion patterns, that if the residual thickness ratio is the same, the residual bearing capacity would be lower than the shear capacity. The research concluded with failure modes of their section included severe local buckling in the bearing stiffener.

3 LTB Moment Capacity: Conventional Approach

3.1 Approach for Assessing LTB

The corrosive effects on the steel plate girders of a bridge don't have any specific guidelines, but to address the impact of corrosive environmental problems on the lateral torsional buckling (LTB), the guidelines of the Eurocode for steel structures will be investigated. The approach for the structural analysis of uniformed corrosive parts will be simulated in software SAP 2000. This should give the opportunity to present an approach for assessing the remaining lateral torsional buckling (LTB) capacity of corroded steel plate girder bridges, with the aim on I-beams.

3.2 Eurocode

The Eurocode is frequently used throughout the thesis, to gather the information needed. It is a set of European standards for design of structures and civil engineering works. The Eurocode provides a unified approach to structural design across Europe, aiming to ensure safety, serviceability, and the durability of buildings and infrastructure. It covers various aspects of structural engineering, and it's divided in different parts, consisting of different materials and different structural cases. The most used standards throughout the thesis, is the Eurocode 3, part 2 [13] and Eurocode 1, part 2 [14].

3.2.1 Eurocode 1

The Eurocode 1, part 2 is about loads on structure with focus on traffic loads on bridges. This part of the Eurocode aims to ensure that bridges and transportation structures are designed to safely withstand loads and actions imposed by vehicular and pedestrian traffic, this to ensure the integrity and longevity of these critical infrastructure assets.

3.2.2 Eurocode 3

The Eurocode 3, part 2 consists of guidelines for design of steel structures with particular emphasis on steel bridges including highway and railway bridges. It aims to ensure that steel bridges are designed and constructed to meet the required safety, serviceability, durability criteria, and providing guidance for the efficient use of materials and resources in bridge construction projects.

3.3 Approach for Structural Analysis

Below is a short description of the programs and different software used throughout the thesis. Software was mainly used to save time, but also to increase accuracy on both dimensions and properties. Hand calculations were used before performing different analyses on the computer, to have an idea of what numbers to expect from the software calculations.

SAP2000

SAP2000 is a widely used structural analysis and design software. It's known for modeling, analyzing, and designing a wide range of structures, including buildings, bridges, towers, and more. In addition, SAP2000 can make simulations with different kinds of loads the structure is subjected to, like wind-, traffic- and other plenty of other loads. With SAP2000, almost all values for the cross-sectional properties can be extracted directly out of the program. Using software makes the calculations much faster, and from there on, properties can be directly inserted into the formulas. When the data from SAP2000 was retrieved, the $M_{b,Rd}$-, M_{cr}- and I_w-value was not considered, but rather calculated manually, as errors occurred when calculating the properties for the abnormal sections.

Skyciv

Skyciv was also used to calculate sections properties. Skyciv is a fast and easy website to calculate loads, moments, and properties on not just cross-sections, but also beams and larger structures. While the SAP2000-calculations were the most accurate, Skyciv was used along the way to check if the calculations matched up.

Autodesk – AutoCAD and Revit

AutoCAD and Revit are both applications from the company Autodesk. AutoCAD was the software of choice for designing the cross-section, as it's not possible to create this form of abnormal section in SAP2000s section designer. In this case, it is a section with three different thicknesses on the flanges. The solution was to design sections in AutoCAD, then to import them into the section designer in SAP2000 as a dxf-file.

Revit is a three-dimensional "building information modelling"-software (BIM). The cross-sections were designed in AutoCAD, then to be imported into Revit, to visualize the dimensions. This could have been done in AutoCAD, but as it is easier to create good visualizations in Revit, it was the preferable option.

Python

Python is a programming language and is commonly used for developing websites and writing codes for applications and programs. The purpose of using Python, was to simplify the way of calculating the buckling resistance of a cross-section, by creating a script that lets the user plot in the sections dimensions and material, and then get the results instantly.

Python was also used for plotting graphs for the different corrosion evolution in rural-, urban- and marine environment. By writing a script that used the corrosion wastage model to calculate corrosion penetration in addition to plotting its graph.

Excel

Microsoft Excel is a spreadsheets-software, that can perform calculations from tables of data. Excel was in this thesis used for simplifying hand calculations, creating formulas to find the different properties of the cross-sections by only plotting in the different dimensions. This was to increase efficiency, by not doing all calculations by hand. In addition, Excel was used for merging the different environment-graphs into one, by putting the values from the python script into a table, and then forming one graph with an overview of all values.

Geogebra

Geogebra is a dynamic mathematics-software, capable of functions such as geometry, spreadsheets and graphing. When using the formula for finding a warping constant, the distance between the shear centers of each flange (h_s) is needed. This was no problem for sections with equally thick flanges, but when calculating the h_s for the section that only corroded on one side, the shear center of the lower flange moved towards the thicker side of the flange. GeoGebra could then be used to plot three different shear centers for the different thicknesses on the flange which formed a triangle, then to use the middle of the triangle to find the shear center.

3.4 Formulas for Calculating LTB

The formulas for determining if there is any (LTB) is shown in these steps shown under:

Step 1. Section classification (1-4 classes) for the effect of local buckling.

Flange (compression):

$$\frac{C_f}{t_f} = ((b - 2r - t_w)/2)/t_f \tag{18}$$

Web (bending):

$$\frac{C_w}{t_w} = (h - 2r - t_f)/t_w \tag{19}$$

Step 2. Design section moment resistance ($M_{c,rd}$) (For yielding).

$$M_{c,rd} = \frac{Wfy}{\gamma M_0} \tag{20}$$

$\boldsymbol{fy = Yield\ strength\ of\ material}$ ($\mathbf{275mpa}$)

$\boldsymbol{\gamma M_0 = Partial\ factor\ for\ material}$ ($\mathbf{1.05}$)

$\boldsymbol{W = W_{pl}(plastic\ section\ modulus) = W_{pl_{flange}} + W_{pl_{web}}}$

$$W_{pl_{flange}} = 2 * (\frac{b_f * t_f^2}{4}) \tag{21}$$

$$W_{pl_{web}} = \frac{b_f * t_w^2 * (d - t_w)}{6} \tag{22}$$

Step 3. Checking for lateral bracings.

$$\overline{\lambda_f} = \frac{k_c L_c}{i_{f,c}\lambda_1} \leq \overline{\lambda_{c0}} \frac{M_{c,Rd}}{M_{y,Ed}} \tag{23}$$

$$\lambda_1 = \pi\sqrt{\frac{E}{f_y}} = 93{,}9\varepsilon \tag{24}$$

$$\varepsilon = \sqrt{\frac{235}{f_y}} \tag{25}$$

$\boldsymbol{k_c = Correction\ factor\ which\ allows\ for\ moment\ distribution}$

$\boldsymbol{i_{f,z} = Radius\ of\ gyration\ about\ z\ axis}$

$\boldsymbol{L_c = Length\ between\ lateral\ restrains}$

$\boldsymbol{\overline{\lambda_{c,0}} = Slenderness\ limit\ (conservative\ 0.3\ or\ less\ 0.5)}$

$\boldsymbol{M_{c,Rd} = Design\ sectional\ moment\ resistance\ for\ fully\ braced\ segment}$

$\boldsymbol{M_{y,Ed} = Maximum\ design\ moment\ in\ the\ segment}$

Step 4. Design buckling resistance moment: Conservative method ($M_{b,Rd}$)

$$M_{b,Rd} = \chi_{lt} W_y \frac{f_y}{\gamma_{M1}} \qquad M_{b,Rd} \leq M_{c,Rd} \tag{26}$$

$$\overline{\lambda_{Lt}} = \sqrt{\frac{W_y\, f_y}{M_{cr}}} \quad \leq 0{,}2 \;\; No\ lateral - torsional\ buckling\ occurs \tag{27}$$

$$M_{cr} = \alpha_m M_{zx} \longrightarrow \; M_{zx} = M_{vio} = \frac{B_1}{L}\sqrt{1 + \frac{B_2^2}{L^2}} \tag{28}$$

$$B_1 = \pi\sqrt{EI_z * GI_T} \qquad B_2 = \pi\sqrt{\frac{EC_W}{GI_t}} \tag{29}$$

$\boldsymbol{I_T = Torsional\ constant}$

$\boldsymbol{I_Z = Moment\ of\ inertia}$

$\boldsymbol{C_W = Warping\ constant}$

$$\chi_{Lt} = \frac{1}{\phi_{Lt} + \sqrt{\phi_{Lt}^2 - \bar{\lambda}_{Lt}^2}} \quad But\ \chi_{Lt} < 1{,}0 \tag{30}$$

$$\phi_{Lt} = 0{,}5[\,1 + \alpha_{Lt}\left(\overline{\lambda_{Lt}} - 0.2\right) + \bar{\lambda}_{Lt}^2\,] \tag{31}$$

$$\alpha_{Lt} = found\ from\ Table.6.3\ in\ "NS - EN\ 1993 - 1 - 1{:}2005 + NA{:}2008" \tag{32}$$

This formulas from the Eurocode shows that to determine LTB, area, moment of inertia, torsional and warping constants must be calculated, to find the final $M_{b,Rd}$. It's quite many steps required to find the LTB, it can even be more if there is any special cases, or relationships between the properties and the dimensions of the section .

4 Corrosion Wastage Model

Corrosion growth is time dependent, and from research its shown that a corrosion propagation can be approximated in a good way by a nonlinear function. In the beginning of the process its assumed that corrosion doesn't influence the material, because of sufficient treatment of the surface of new steel members. After the first sign of corrosion appears, there will be a nonlinear process of growth over time initiated as followed [22]:

$$C(t) = A(t - t_0)^B \; ; t > t_0 \tag{33}$$

$C(t)$: average corrosion penetration in millimeters

t: age in years

t_0: time in years of first appearance of the sign of general (uniform) corrosion

Table 1: Parameters for *A* and *B* in wastage model

Environment	*Carbon steel*		*Weathering steel*	
	A(mm)	*B*	*A(mm)*	*B*
Rural	0.0340	0.650	0.0333	0.498
Urban	0.0802	0.593	0.0507	0.567
Marine	0.0706	0.785	0.0402	0.557

It's shown in most cases that rural environments have lower degree of penetration than in the marine environments. This because of sea water hawing a big impact on corroded elements.

The time-dependent reduction of cross-sectional area of the member is calculated considering the reduction of plate thickness due to general corrosion wastage, with the following equations [18].

$$A_{eff}(t) = A_0 - \sum_{i=1}^{n} C_i(t) l_i \tag{34}$$

A_{eff} represents the area after being reduced.

5 LTB Moment Capacity of Corroded Steel Bridges: Proposed Framework

A framework based on essential guidelines from Eurocode for calculating LTB, alongside the wastage model. Together, these two forms the guidelines towards making a prediction for estimating the future of LTB capacity due to corrosion.

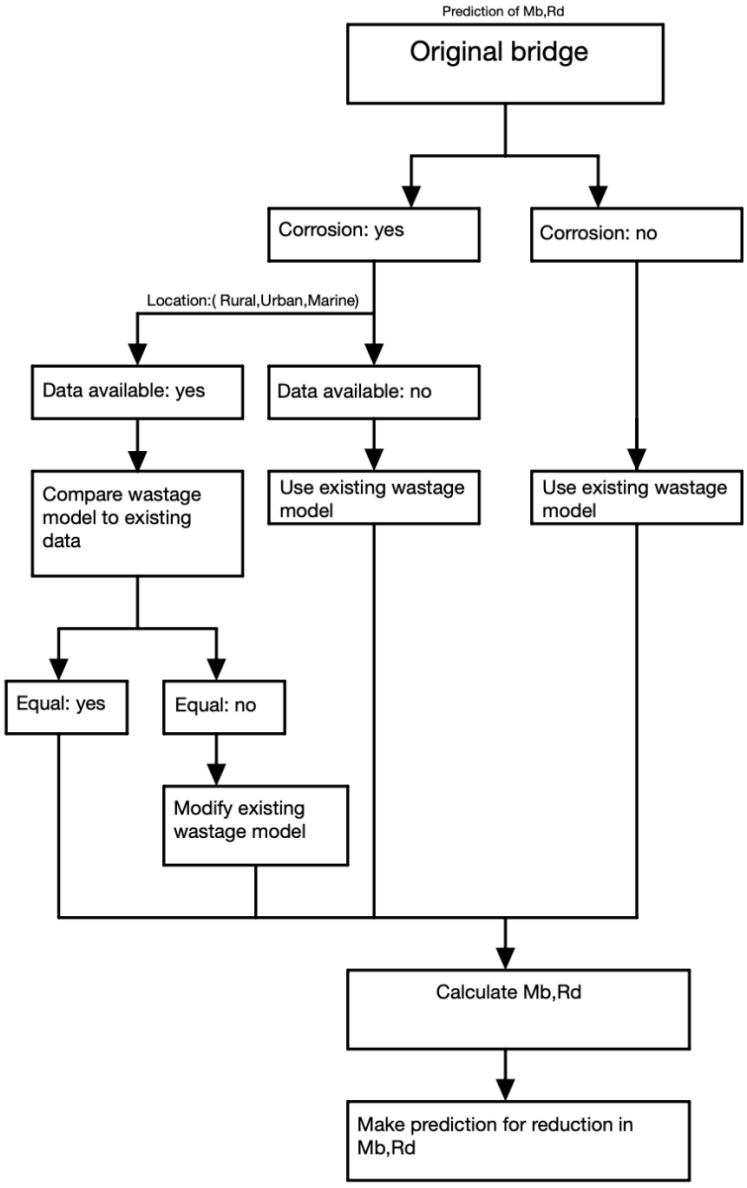

This framework shows the steps towards figuring out LTB capacity considering the research done in this thesis.

6 LTB Moment Capacity of Corroded Steel Bridges: A Case Study

6.1 Considered Bridge

The bridge is called Storåna I and was constructed in 1937. It is located in Årdal, Hjelmeland municipality in Norway, an approximately 50-minute-long drive from the city of Stavanger. There is a view of the bridge shown in Figure 4. Storåna I was partially destroyed by floods and was rehabilitated and rebuilt in 1942 with the modifications it has today. The bridge is a part of the Rv13 national road and leads a pathway over the Storåna river and is therefore surrounded by a corrosive environment. Due to road traffic, different values of live load are frequently subjected to the bridge.

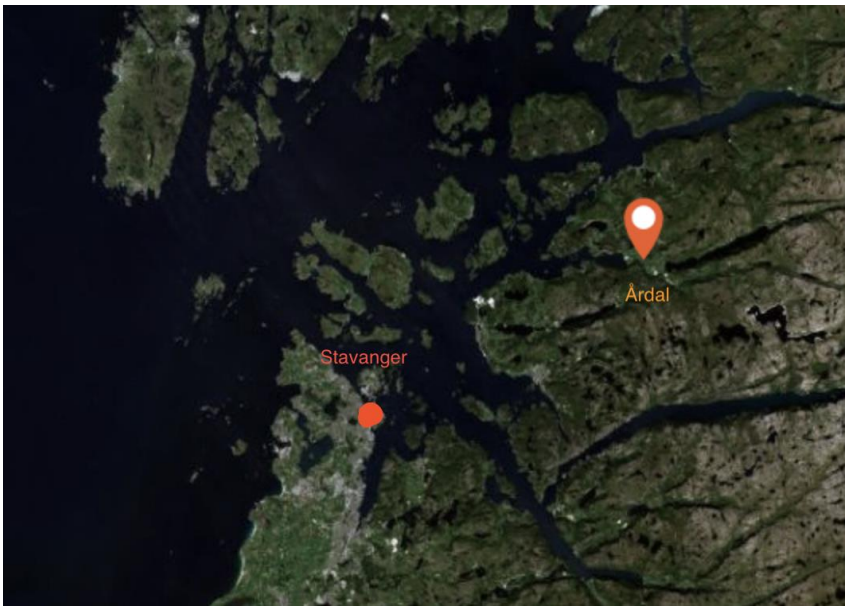

Figure 3: Bridge location

Figure 4: Storåna I bridge

6.1.1 Geometrical Information and Material Properties

The existing Storåna I bridge has one end span of concrete T-beams with 12.7 m length, and two simple spans of non-composite sections, where both have an equal length of 19.8m. There is a two-lane single carriageway and superstructure is supported by two pillars. The non-composite section consists of a reinforced concrete deck founded on a girder. The section consists of three evenly spaced rolled steel girders, designed as DIP 95. The total width of the concrete slab is 5.82m, with an average depth of 190mm. The section consists of a web connected to two flanges, one on top, and one on the bottom. The flanges connect to the web via a fillet with a radius of 30mm. The three main steel girders with depth, web thickness, flange width and flange thickness 950mm, 19mm, 300mm and 36mm respectively.

6.1.2 Damage and Defects of the Steel Bridge

The bridge has had inspection reports, and visual inspection that concludes with observed coating loss and corrosion in the bridge girders due to the age of the bridge, increased load cycles, and exposure of corrosive environment. There is reported that the bridge is exposed to uniform/patch corrosion. From the report there was no visual cracks in the steel parts of the bridge. There was found a maximum of 4mm uniform corrosion in the midspan of the exterior girder. Under inspection it is found that the corrosion was on the bottom surface of the top flange, and on the bottom and top surface of the bottom flange. Fillets are supporting the webs, connecting them to the flanges. These will also be affected by corrosion, and even though their radii doesn't change, they are still suffering from material loss.

The corrosion damage will have an impact on the geometric properties of the structural behavior of steel. This may especially affect the lateral torsional buckling of the steel girders.

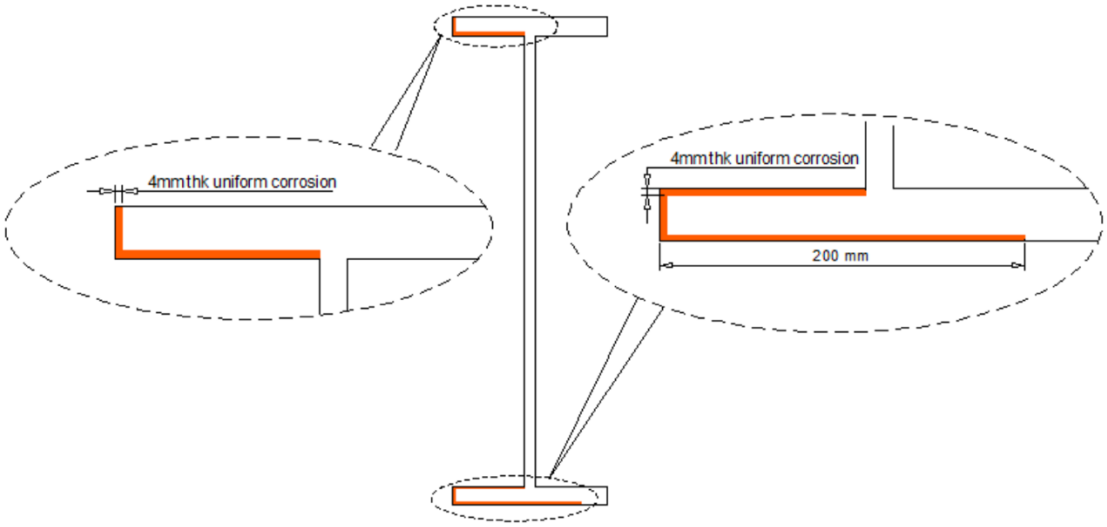

Figure 5: Corroded member [1]

The documents of the inspection reports and existing drawings of the bridge is made by "Statens vegvesen" and will be found in Appendix A.

6.1.3 Cross-Sectional Properties of Uncorroded Beams

Table 2: Properties of I-beam

Steel beam section:	DIP 95
Structural steel:	S275
f_y	275 MPA
E	20 GPA
Depth of section (H)	950 mm
Width of section (B)	300 mm
Web thickness (t_w)	19 mm
Flange thickness (t_f)	36 mm
Fillet radius (r)	30 mm

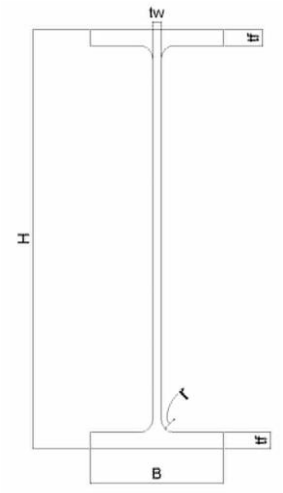

Figure 6: Dimensions

HE-A		Dimensjoner					Masse	A	A steg	y-y			z-z			It	Sy	Cw
		h	b	s	t	r				I	W	i	I	W	i			
		mm	mm	mm	mm	mm	kg/m	mm^2		I*10^-9mm	mm^3	mm	I*10^-9mm	mm^3	mm			
HE-A																8250	6410	32074
400	HEA400	390	300	11	19	27	125	15900	3872	0,4507	2310000	168	0,0856	571000	73,4		1280000	
550	HEA550	540	300	12,5	24	27	166	21200	6150	1,119	4150000	230	0,1082	721000	71,5		1970000	
600	HEA600	590	300	13	25	27	178	22600	7020	1,412	4790000	250	0,1127	751000	70,5		2680000	
650	HEA650	640	300	13,5	26	27	190	24200	7938	1,752	5470000	269	0,1172	782000	69,7		3070000	
700	HEA700	690	300	14,5	27	27	204	26000	9222	2,153	6240000	288	0,1218	812000	68,4		3520000	
800	HEA800	790	300	15	28	30	224	28600	11010	3,034	7680000	326	0,1264	843000	66,5		4350000	
1000	HEA1000	990	300	16,5	31	30	272	34700	15312	5,538	11190000	400	0,14	934000	63,5		6410000	
									0									
DIP									0									
32	DIP32	320	300	13	22	20	135	17100	3588	0,3225	2020000	137	0,0991	661000	76		1130000	
42,5	DIP42,5	425	300	14	26	21	166	21200	5222	0,6948	3270000	181	0,1171	781000	74,3		1830000	
45	DIP45	450	300	15	28	23	182	23200	5910	0,8422	3740000	190	0,1262	841000	73,8		2120000	
50	DIP50	500	300	16	30	24	200	25500	7040	1,132	4530000	210	0,1353	902000	72,8		2560000	
55	DIP55	550	300	16	30	24	207	26300	7840	1,403	5100000	231	0,1353	902000	71,7		2880000	
60	DIP60	600	300	17	32	26	227	28900	9112	1,808	6030000	250	0,1444	962000	70,7		3500000	
65	DIP65	650	300	17	32	26	234	29700	9962	2,168	6670000	270	0,1444	962000	69,7		3780000	
75	DIP75	750	300	18	34	27	261	33300	12276	3,163	8430000	308	0,1535	1020000	67,9		4800000	
80	DIP80	800	300	18	34	27	268	34200	13176	3,664	9160000	327	0,1535	1020000	67		5220000	
85	DIP85	850	300	19	36	30	292	37200	14782	4,439	10440000	346	0,1627	1080000	66,1		5980000	
90	DIP90	900	300	19	36	30	299	38100	15732	5,06	11250000	364	0,1627	1080000	65,3		6450000	
95	DIP95	950	300	19	36	30	307	39100	16682	5,73	12060000	383	0,1627	1080000	64,5		6930000	
100	DIP100	1000	300	19	36	30	314	40000	17632	6,447	12900000	401	0,1627	1080000	63,7		7430000	
									0									
DIMAX									0									
90	DIMAX90	908	302	21	40	30	332	42300	17388	5,676	12500000	366	0,1845	1220000	66		7040000	
100	DIMAX100	1008	302	21	40	30	349	44400	19488	7,23	14330000	403	0,1846	1220000	64,5		8092000	

Figure 7: Table for beam dimensions

6.2 Calculation of LTB Moment Capacity

6.2.1 Case 1. Method 1: No Corrosion Case with Simplified Approach

The first case is a simplified approach for determining LTB. beam cross-section DIP 95 with no corrosion. This method is used for fast calculations. This method uses pre-defined values from a buckling curve to calculate $M_{b,\,Rd.}$ The simplified approach can give a wrong answer, as one must be very precise when picking pre-defined value from the buckling curve showed under:

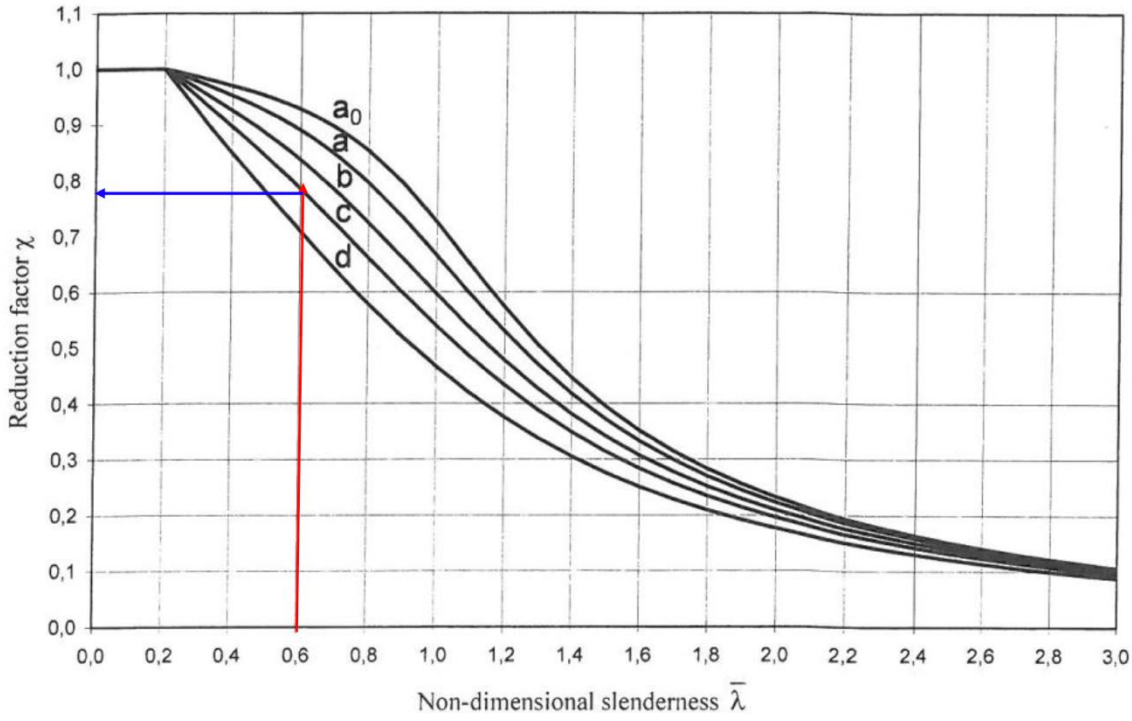

Figure 8: Buckling curves [16]

Since the beam span is 19800mm (Lc), and there are no bracings on it, the lambda-value $(\overline{\lambda})$ in the buckling curve is noticeably high. This gives a reduction factor (X) of approximately 0.15, which gives a $M_{b,Rd}$ of 412.7 kNm.

- **$M_{b,Rd}$= 412.7 kNm**

6.2.2 Case 1. Method 2: No Corrosion Case with Conservative Approach

Method 2 is a method for calculating LTB for the same cross-section as in method 1 (no corrosion), but with a more conservative approach. This method includes considering the torsional and warping constant into the calculations. This approach takes longer time but gives a more accurate answer than the simplified approach.

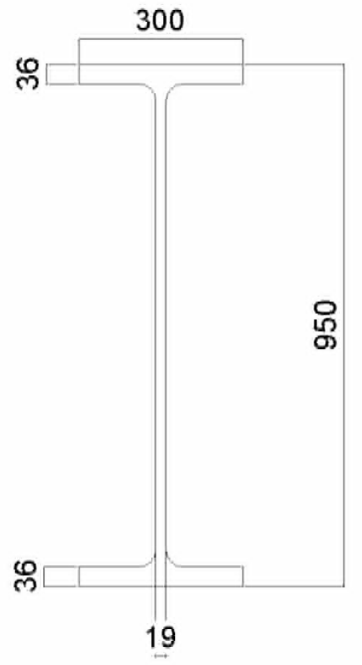

Figure 9: No corrosion

Table 3: Results of no corrosion

DIP95 – No corrosion			
A	39100.85	S_y	12080032
I_{y-y}	5.738*10^9	S_z	1085015.4
I_{z-z}	1.628*10^8	$W_{pl,y-y}$	13886688.43
A_{y-y}	21953.562	$W_{pl,z-z}$	1712702.976
A_{z-z}	17724.94	K_{y-y}	383.0785
I_t	11420909	K_{z-z}	64.5165
I_w	3.399*10^6	$M_{c,Rd}$	3636.99
M_{cr}	1101.73	$\overline{\lambda}_{LT}$	1.862
ϕ_{LT}	2.864	χ_{LT}	0.198
h_s	914	$M_{b,Rd}$	721.4

When calculating $M_{b,Rd}$, the properties of the cross-section is found by the software SAP2000. The different properties are then inserted into the formulas included in chapter 3.4 This gave a significantly higher $M_{b,Rd}$ than when using simplified method.

- **$M_{b,Rd}$ = 721.4 kNm**

6.2.3 Case 2. Uniform Corrosion Symmetric Approach

Case 2 uses the same conservative approach as in case 1, method 2. The cross-sectional area of the I-section has been drastically reduced in this case. The section has been reduced by 4mm on the whole of the lower flange, the sides and "beneath" the upper flange. In addition to this, the fillets will now be smaller, even though they still have the same radius, which will make the upper and lower parts of the web its thinnest area. This to have an extreme loss of area, and to make the calculations easier as the cross-sections left- and right side still is identical.

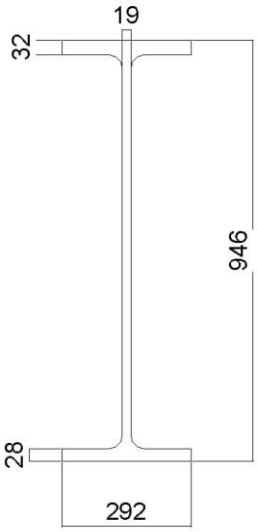

Figure 10: Corrosion on both sides

Table 4: Results of corrosion on both sides

DIP95 – Corroded on both sides			
A	35067.31	S_y	10120574
I_{y-y}	4.906*10^9	S_z	857507.332
I_{z-z}	1.252*10^8	$W_{pl,y-y}$	12047481.93
A_{y-y}	18098.499	$W_{pl,z-z}$	1370319.565
A_{z-z}	17584.677	K_{y-y}	374.2249
I_t	7420361.333	K_{z-z}	59.6722
I_w	2.611*10^13	$M_{c,Rd}$	3155.29
M_{cr}	790.343	$\overline{\lambda}_{LT}$	2.047
ϕ_{LT}	3.29	χ_{LT}	0.169
h_s	916	$M_{b,Rd}$	536.3

This section also gets different properties from the software SAP2000. Since the cross-section still is equally thick on each side, the software calculates the properties, which gives a $M_{b,Rd}$ = 536.3 kNm. In comparison, the simplified method gives a $M_{b,Rd}$ =377.14 kNm.

- **$M_{b,Rd}$ = 536.3 kNm**

6.2.4 Case 3. Uniform Corrosion with Asymmetric Approach

Case 3 consists of a cross-section that's not symmetric in any aspect. The approach is still the same as in case 1 and case 2 for finding LTB, but some calculations of the properties are different. This because of the asymmetrical dimensions. On the upper flange, there is now a 4mm deep corrosive attack on the left side, as well as beneath all the way to the web. On the lower flange, the top is undergoing the same depth of corrosion from the lower part of the web, through the fillet and all the way to the edge, affecting the left side. Underneath the flange, the corrosion continues 196mm towards the right side.

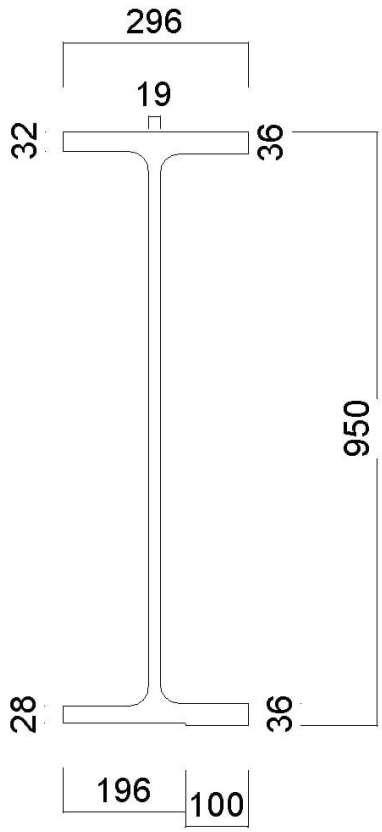

Figure 11: Asymmetric corrosion

Table 5: Result of asymmetric corrosion

DIP95 – Corroded asymmetric			
A	37980.27	S_y	11302666
I_{y-y}	5.479*10^9	S_z	955807.2
I_{z-z}	1.437*10^8	$W_{pl,y-y}$	13342887
A_{y-y}	20951.117	$W_{pl,z-z}$	1559628.2
A_{z-z}	18017.166	K_{y-y}	379.8189
I_t	12552020	K_{z-z}	61.5049
I_w	3.0160*10^13	$M_{c,Rd}$	3494.57
M_{cr}	1068.058	$\overline{\lambda}_{LT}$	1.853
ϕ_{LT}	2.846	χ_{LT}	0.199
h_s	916.26	$M_{b,Rd}$	698.1

As the software had difficulties calculating some values, such as the warping constant, this had to be done manually. The warping constant is necessary for calculating the buckling resistance manually, and to find the warping constant, a H_s-value is needed. Figure 12, shows the work done in Geogebra to extract the H_s-value. When extracted, the calculation of the $M_{b,Rd}$ was possible, which gave a value of 698.1 kNm. For comparison, the simplified method in case 3 gave a $M_{b,Rd}$ =396.53 kNm

$M_{b,Rd}$ = 698.1 kNm

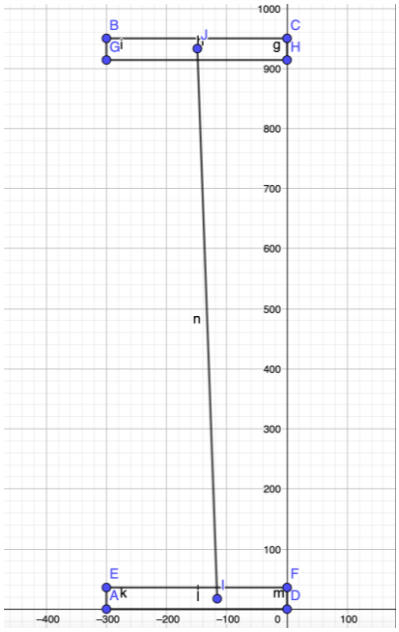

Figure 12: H_s of asymmetric corroded beam

6.2.5 LTB with Bracings

The blueprint for the bridge shows a 19.8 m span, which was considered in the previous cases. This sounded unnatural, so after guidance from supervisor, bracings was instated at two points along the span; at each 6.6 meters. (19.8/3)

When calculating with bracings along the span, the only change in the calculations, was changing the L_c from 19.8 to 6.6. The $M_{b,Rd}$ for each case was calculated for comparison.

	Case 1	**Case 2**	**Case 3**
$M_{b,Rd}$ (kNm)	1950.759	1572.354	1838.63

7 Corrosion Degradation Status

7.1 Comparison of Existing Wastage Model with Current Degradation Status

7.1.1 Degradation of a Lifespan of 87 Years

From the existing rapports of the "Storåna" bridge, there is discovered that the current degradation is shown to be 4mm of uniform corrosion on the cross-section. When comparing the existing wastage model from Chapter 4, there are some issues with the current model compared to the discovered situation. In the following graphs, corrosive penetration for the three different environments is calculated for the current lifespan of 87 years (1937-2024).

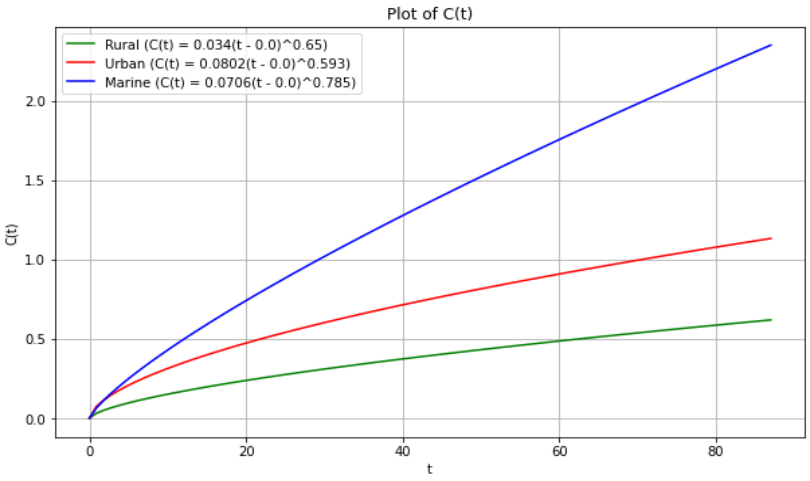

Figure 13: Wastage model 87 years

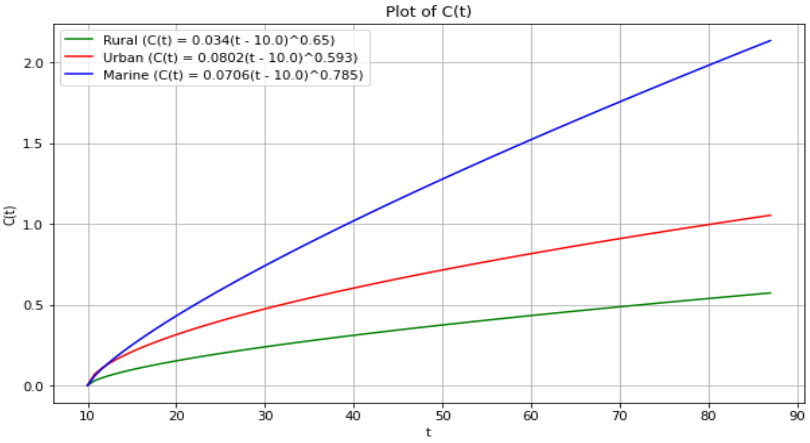

Figure 14: Wastage model 77 years

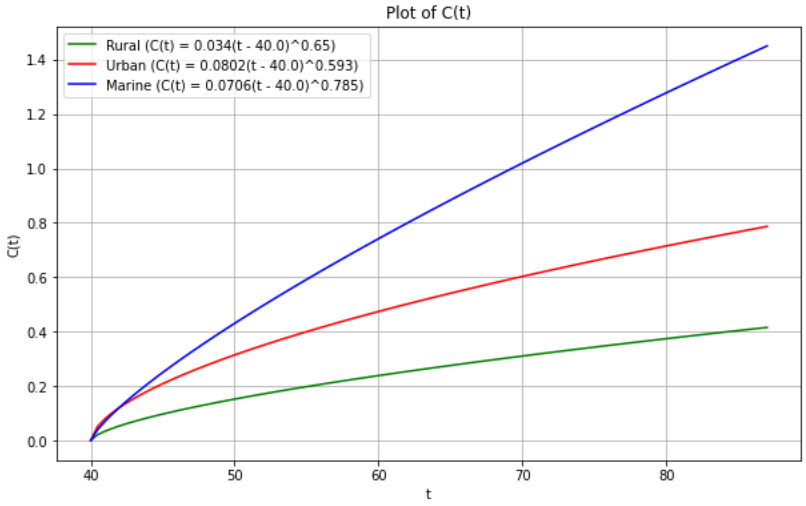

Figure 15: Wastage model 47 years

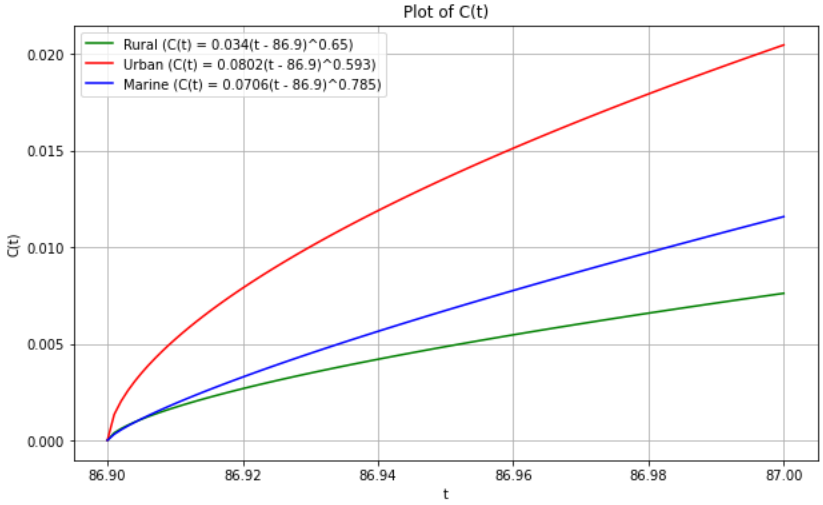

Figure 16: wastage model beginning

Table 6: Values of degradation after 87 years

Year(s) before corrosion start	Rural (Green)	Urban (Red)	Marin (Blue)
0	0.6197	1.1332	2.3514
10	0.5724	1.0541	2.1365
40	0.4153	0.7866	1.4501
86.9	0.0076	0.0205	0.0116

The theoretical degradation from the wastage model is shown in the table above in millimeters. The bridge is sited in a rural environment, and should after the current wastage model be around 0.6197 mm. This shows that the current wastage model gives a way smaller prediction of the degradation than what is reported.

External factors like the coating of steel, and salt from de-icing the roads may be some of the reason for this big deviation. The coating of steel often has a life expectancy of 5-10 years. The result from the table above shows that the simulated corrosion in a marine environment (2.3514mm) is closer to the discovered corrosion than in a rural environment (0.6197mm), although still far from 4mm.

7.1.2 Degradation of a Lifespan of 120 Years.

To further investigate the simulated degradation for the future, the graphs are now extended to simulate 120 years.

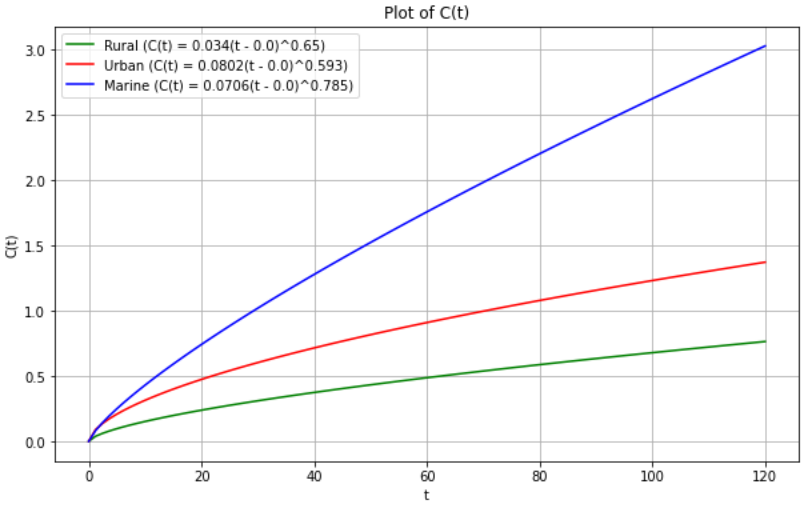

Figure 17: Wastage model of 120 years

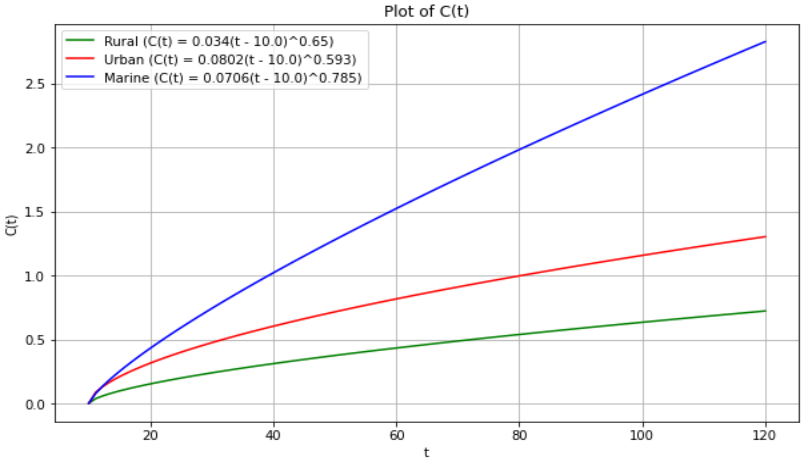

Figure 18: Wastage model with 10 years before corrosion

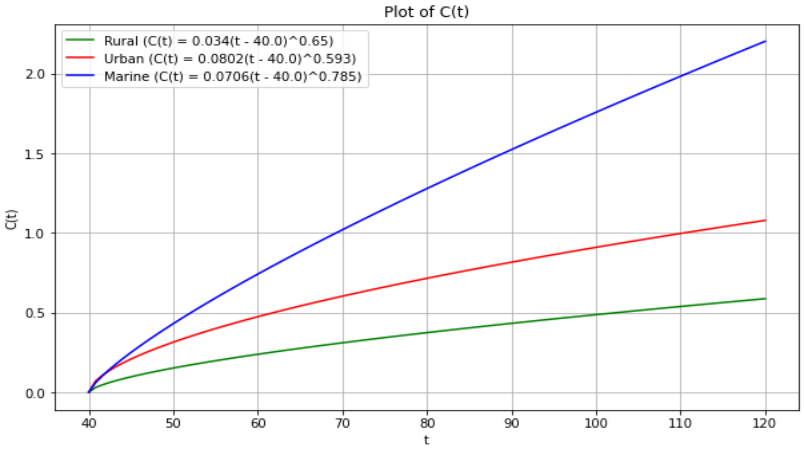

Figure 19: Wastage model with 40 years before corrosion

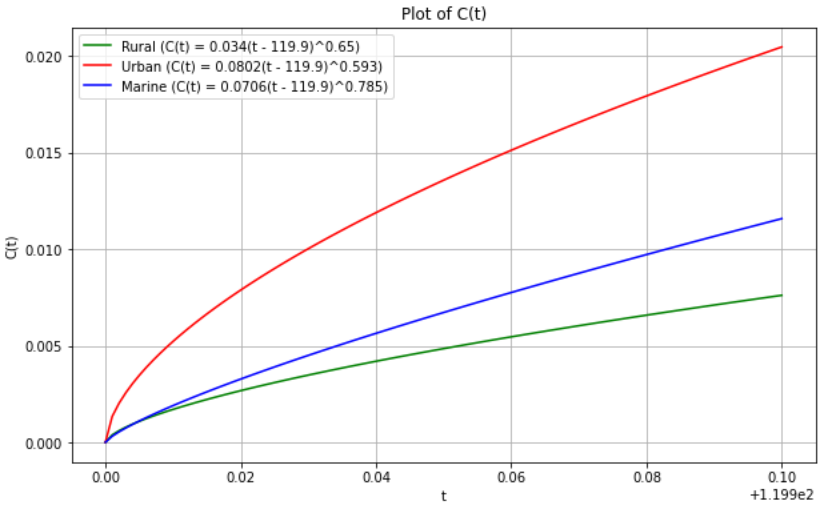

Figure 20: wastage model from the beginning

Table 7: Values of degradation after 120 years

Year(s) before corrosion start	Rural (Green)	Urban (Red)	Marine (Blue)
0	0.7637	1.3713	3.0266
10	0.7217	1.3023	2.8268
40	0.5868	1.0782	2.2016
119.9	0.0076	0.0205	0.0116

The values from Table 7 shows that the corrosion after 120 years (0.7637mm) is still way lower than the reported values. The corrosive degradation in marine environment (3.0266mm) is getting close to the reported penetration.

7.1.3 Corrosion Degradation Status

Corrosion degradation can also be approached in a more linear way, according to A. Aeran et al. [23], C(t)=At, where A is 0.3. Using the same lifespans, with corrosion from the beginning, after 10 years, after 40 years, and after 120 years to show the difference.

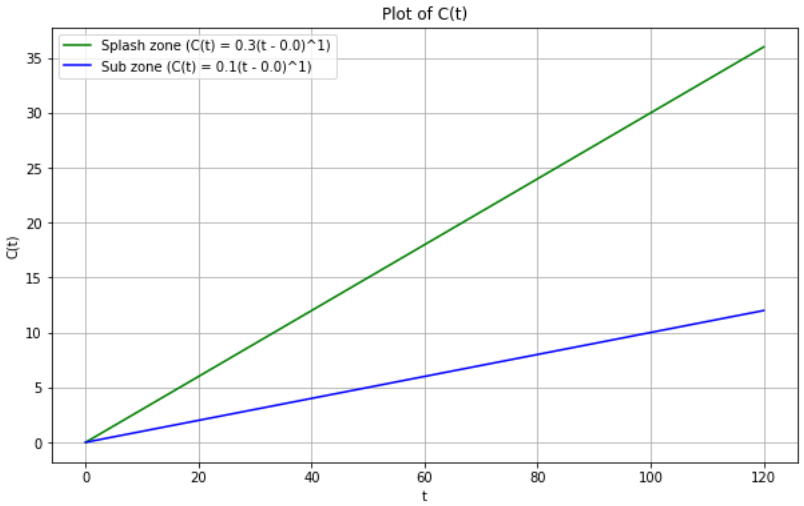

Figure 21: Wastage model for offshore structures 0 years

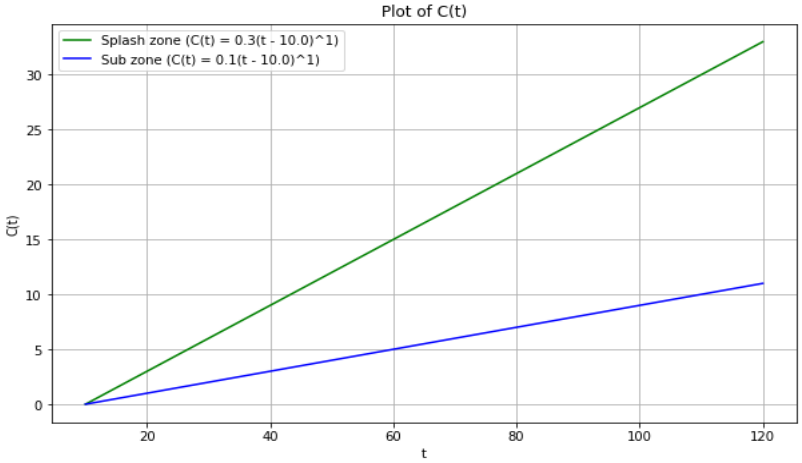

Figure 22: Wastage model for offshore structures 10 years

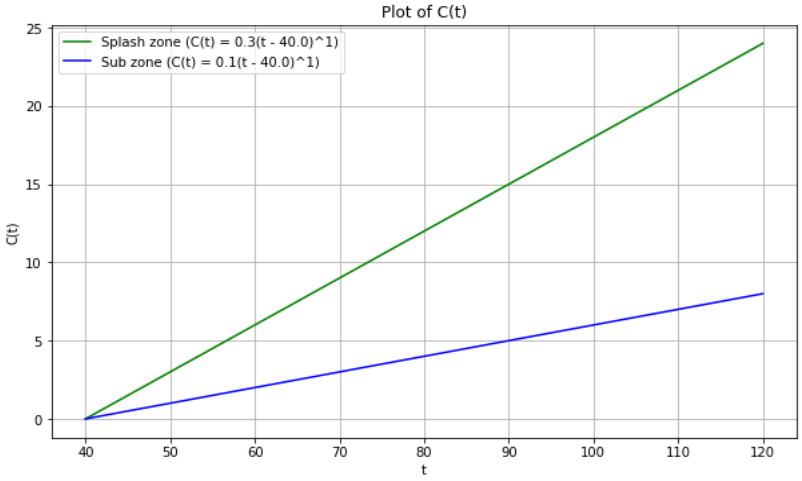

Figure 23: Wastage model for offshore structures 40 years

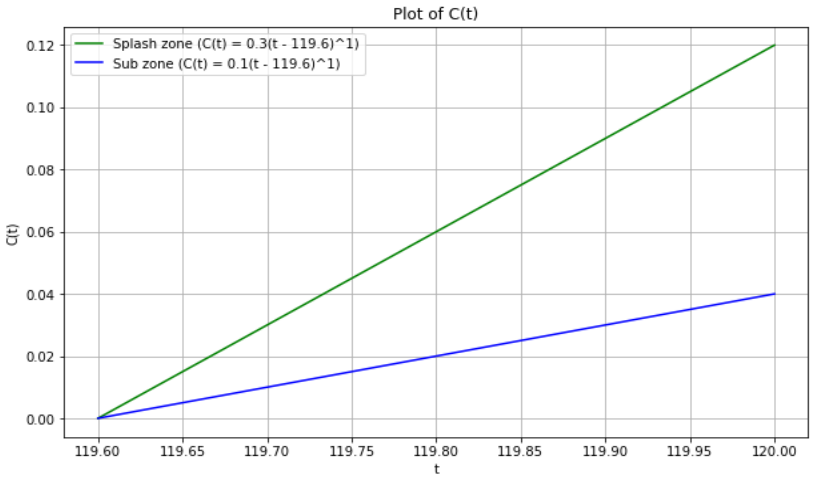

Figure 24: Wastage model for offshore structures 120 years

Table 8: Values of degradation after 120 years (linear approach)

Year(s) before corrosion start	Splash zone (Green)	Sub zone (Blue)
0	36	12
10	33	11
40	24	8
119.9	0.12	0.04

Table 8 illustrates much higher values than with the wastage model. This approach is mainly used for offshore structures, which undergoes much more extreme conditions, than if placed in a rural site.

7.1.4 Proposed Degradation Model

To force the corrosion state of 4mm degradation after 87 years, tweaking the B-value is necessary to get the decrease in area right. Since marine areas has the highest degradation when analyzing over several years, it is the best degradation line to follow. To get a corrosion penetration of 4 mm, the B-value of the marine degradation line must be at 0.903964, but as the bridge is localized in a rural environment, it is still included as a line for comparison. The B-value for the rural environment must be tweaked to 1.0675745 to get a corrosion of 4mm, but as the value is over 1 it is not considered. The marine degradation line is used instead, since with a B-value of under 1, its penetration will decrease in the long run.

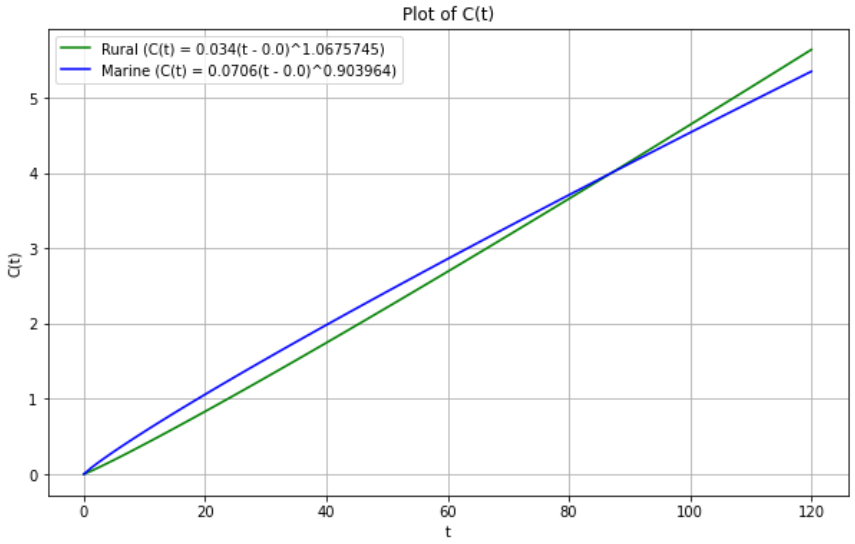

Figure 25: Degradation with tweaked B-values

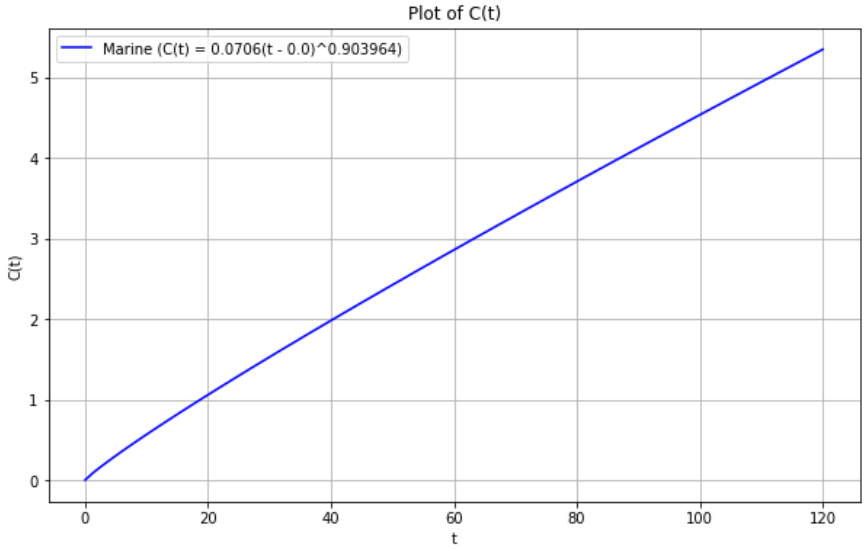

Figure 26: Degradation with tweaked B-values: only marine

Table 9: Predictions of values of degradation for 100 and 120 years

Year	Rural (Green)	Marine (Blue)
100	4.6412	4.5366
120	5.638	5.349

Table 9 shows a prediction for the corrosive penetration after 100 and 120 years, with the tweaked B-values. After 100 years its predicted to be a uniform corrosion of 4.54 mm and after 120 years its predicted to be a uniform corrosion of 5.35 mm.

7.2 Prediction of Buckling Capacity Degradation

With the predictions from the wastage model, the LTB capacity curves for 100 and 120-years can be made. The values in Table 10 and Table 11 are made from using the same asymmetric figure but reducing to 4.5366 mm and 5.349 mm instead of 4 mm.

Table 10: Predictions of Mb,Rd after 100 years

DIP95 – Corroded asymmetric after 100 years (4.5366 mm)			
A	37635	S_y	11125879
I_{y-y}	5.409*10^9	S_z	937945.5
I_{z-z}	1.411*10^8	$W_{pl,y-y}$	13186015
A_{y-y}	20613.321	$W_{pl,z-z}$	1535784.2
A_{z-z}	17993.688	K_{y-y}	379.0977
I_t	12091432	K_{z-z}	61.2253
I_w	2.9600*10^13	$M_{c,Rd}$	3453.48
M_{cr}	1040.171	$\overline{\lambda}_{LT}$	1.867
ϕ_{LT}	2.876	χ_{LT}	0.197
h_s	916.04	$M_{b,Rd}$	681.9

The $\mathbf{M_{b,Rd}}$ should be approximate **681.9 kNm** after the bridges life time passes **100 years**, considered the research and the new wastage model with the marine degradation line.

Table 11: Predictions of Mb,Rd after 120 years

DIP95 – Corroded asymmetric after 120 years (5.349 mm)			
A	37209.84	S_y	10895450
I_{y-y}	5.319*10^9	S_z	911897.7
I_{z-z}	1.372*10^8	$W_{pl,y-y}$	12989273
A_{y-y}	20193.101	$W_{pl,z-z}$	150268.1
A_{z-z}	17974.451	K_{y-y}	378.0941
I_t	11656942	K_{z-z}	60.7303
I_w	2.8802*10^13	$M_{c,Rd}$	3401.95
M_{cr}	1007.739	$\overline{\lambda}_{LT}$	1.882
ϕ_{LT}	2.911	χ_{LT}	0.194
h_s	916.37	$M_{b,Rd}$	662.8

The **$M_{b,Rd}$** should be approximate **662.8 kNm** after the bridges life time passes **120 years**, considered this research and the new wastage model with the marine degradation line.

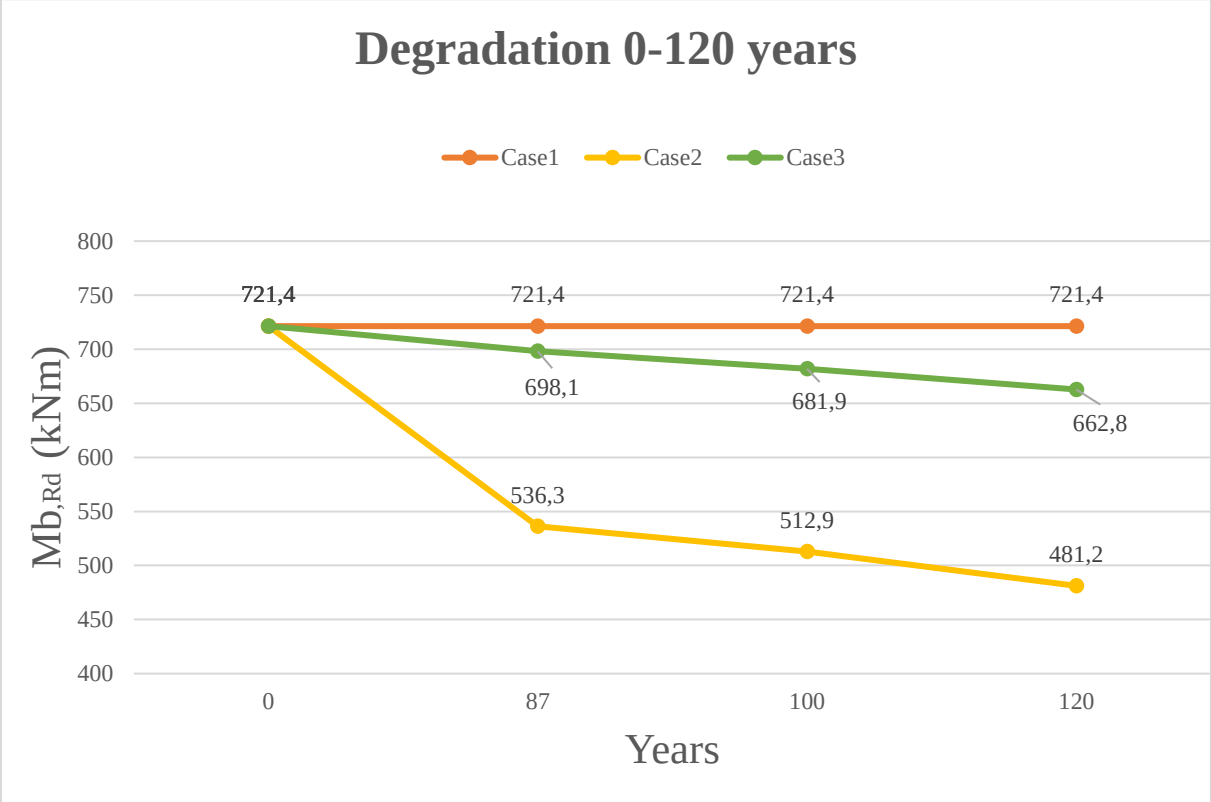

Figure 27: Decrease of Mb,Rd

The graph above shows the three different cases used throughout the thesis. **Case 1** shows the steel-beam when there is no corrosion. This gives a straight line as there is no change in calculations. **Case 2** is uniform corrosion; this gives a more drastic reduction as area is reduced at both top and bottom. This is not a realistic behavior of corrosion, but gives a god perspective of the area loss compared to the reduction in $M_{b,Rd}$. **Case 3** is the real reduction of the cross-section, and gives a prediction of the future reduction of the $M_{b,Rd}$ if the corrosive attack is distributed over the same areas as today (87 years). This gives a prediction of how much $M_{b,Rd}$ will be reduced in the bridges designed life span. The graph shows a prediction of 5.47% reduction of $M_{b,Rd}$ during 100-years, based on the reported knowledge of 4 mm of corrosion degradation after 87 years.

8 Results and Discussion

8.1 Reduction of LTB Moment Capacity with Loss of Area

There is a clear link between area and the $M_{b,Rd}$, when studying the reduction of $M_{b,Rd}$ due to area loss. The reason for investigating the area loss is because moment of inertia-, warping- and torsional constant depends on the cross-sectional area.

Table 12: Comparison of area loss and reduction of $M_{b,Rd}$

Case:	Area: (cm^4)	Reduction: (cm^4)	%	$M_{b,Rd}$: (kNm)	Reduction, from method2 (kNm)	%, From method2
Case 1, Method 1	391.0085	0	**0**	412.7	308.7	**42.79%**
Method 2	391.0085	0	**0**	721.4	0	**0%**
Case 2: 87-year	350.6731	40.3354	**10.31%**	536.3	185.1	**25.65%**
100-year	345.1395	45.8690	**11.73%**	512.9	208.5	**28.90%**
120-year	337.1399	53.8686	**13.78%**	481.2	240.2	**33.29%**
Case 3: 87-year	379.8027	11.2058	**2.86%**	698.1	17.8	**3.22%**
100-year	376.35	14.6584	**3.75%**	681.9	39.5	**5.47%**
120-year	372.0984	18.9101	**4.84%**	662.8	58.6	**8.12%**

From Table 12, case 2 shows an extreme case in this scenario, the 10.31% decrease in area makes a 25.65% decrease in the $M_{b,Rd.}$ The numbers can be compared with the research paper written by A. Bao et al.[12], where it is found that a 10% reduction in web thickness may give a 25% or more reduction in buckling capacity. From case 3, the corroded asymmetric cross-section has a reduction of 2.86% in area, and 3.22% in reduction of $M_{b,Rd.}$ This shows a clear relation between area and buckling resistance moment. After 100 years, the table shows a $M_{b,Rd}$-reduction of 5.47%, and 8.12% after 120 years, compared to the original $M_{b,Rd}$ with no corrosion on the steel-girder.

These numbers are based on following the Eurocode for calculating Lateral torsional buckling capacity, including the known knowledge of the existing degradation of 4mm of the bridge. Using this with the

remodeled work of the wastage model from Y. Sharifi and J. K.Paik [22], it is possible to predict the reduction after 100 and 120-years, based on the known corrosion after 87-years.

Compared to the $M_{b,\ Rd}$, the reduction in area is somehow exponential, as shown in Table 12. This indicates that as the corrosion keeps getting deeper into the structure over time, the reduction in $M_{b,Rd}$ will increase, meaning that the risk of failure also increases.

8.2 Discussions

The significant disparity observed between reported corrosion and the predictions generated by the wastage model, which yield substantially lower values is questioning. Contemplation on this matter gravitates towards external factors. For instance, under conditions of strong winds, steel elements may be subjected to impact akin to “blows”, potentially leading to the deeper penetration of particles into the steel and thereby expediting the progression of corrosion.

A concern about the wastage model is that the calculations give a way smaller value than what’s discovered on the bridge. The wastage model should give a larger value of corrosion penetration, as it is safer.

In Table 6, the calculations gave a corrosion penetration of 0.6 mm. Compared to the discovered 4 mm of corrosion penetration on the bridge. In chapter 7.1.4, the B-value in the wastage model was tweaked to match the discovered penetration on the bridge (4mm). The A-value was not changed, to keep a reference point to the original wastage model. The A-value could have been tweaked instead, but as it also represents the cross-sectional area, the B-value is a more preferable option.

Another thing to consider is the placement of the site. Norway undergoes all types of weather throughout a year, which can impact degradation in different ways. This may make the wastage model vulnerable, compared to another place in the world where the weather doesn’t change as much. A specific example of this, is how they de-ice the roads in Norway during the winter, using salt. This emphasizes the importance of continuous observation of corrosive attacks. And to have a good maintenance plan for the steel members, especially as many bridges are closing in on their life expectancy.

For further work, the comparison of the wastage model to a specific case with more data of the corrosion degradation over time should be investigated. This to make a more accurate line between the wastage model and the real corrosion. There should also be more comparison of different settings as this may have an impact of the results.

Comparing $M_{b,Rd}$ to the $M_{y,Ed}$ of a steel bridge can be a good way of measuring how much corrosion the section tolerates before yielding to normal loads such as traffic load. This will also be a good indicator for when the bridge needs replacement or maintenance.

In the last part of chapter 6.2.5, $M_{b,\,Rd}$ for all cases were calculated, included bracings along the beam. This showed a significant increase in buckling resistance, and it could be of good guidance to how to maintain the bridge in the future and expand its lifespan even if it is subjected to a corrosive attack or not.

8.3 Challenges

One of the first problems in the thesis was figuring out the right formulas for $\boldsymbol{I_w}$, $\boldsymbol{I_t}$ and $\boldsymbol{I_z}$ as this is among the most important and most difficult values to figure out for calculating $M_{b,\,Rd}$. Most of the difficulties started with the fillet radius, as it wasn't included in the formulas found at first. This made it problematic checking if the software was calculating the right values. Also, some of the values calculated in the software ended up being zero, due to the abnormal section.

When calculating case 3, h_s was manually calculated on the asymmetrical section. The cross-section into needed to be divided into many squares to find the distance between the shear centers of the flanges. This started out with many unnecessary calculations, before figuring out a way to use GeoGebra to find the correct value.

9 Conclusions

The issue surrounding corrosion on steel beams is of significant importance and warrants further exploration. By examining the relationship between corrosion on a steel beam in a bridge and its impact on lateral torsional buckling capacity, this study has delved into a facet of the field that has not been extensively explored previously. Through this approach and consideration of the issue, alongside other scholarly articles addressing similar instances, particularly one concerning development of corrosion over time , the following conclusions have been reached.

Some of the formulas derived previously don't match with real-world cases. In chapter 7, the formulas derived in other papers give a quite large difference from real life. In this specific case, there is by calculations, 0.6 mm of corrosion compared to 4 mm that has been reported on the bridge. To implicate the formula to this specific case, adjustment of the fixed factors was acquired. With the proposed wastage model, there is an opportunity to estimate what the corrosion can be in the future, and with these new values, there is also a possibility to calculate lateral torsional buckling capacity of the bridge in the future. This can be a way to determine when the bridge needs to be replaced. In conclusion, the proposed framework and methodology demonstrated in this case study can be effectively employed to forecast the time-dependent degradation of lateral torsional buckling moment capacity of steel plate girder bridges under uniform corrosion.

The challenges associated with corrosion are multifaceted. Each case present unique complexities, influenced by various factors. The location and environmental conditions surrounding a particular site play significant roles, making it difficult to formulate a one-size-fits-all guideline. This underscores the importance of further research into the corrosion aspect of engineering. Certain regions, such as those characterized by dry climates, experience less susceptibility to corrosion. In this scenario, there was an attempt to apply an existing degradation model tailored for rural environments that is reflecting the placement of the bridge. However, it's evident that insufficient maintenance may have contributed to deviation from the predicted degradation pattern. Furthermore, there may be additional unaccounted factors at play, such as the impact of the de-icing process during winter periods.

References

[1] MT Gebremeskel, AT Cruz (2022) *Fatigue life assessment of a steel bridge based on measured corrosion wastage and actual traffic loading*, Master`s Thesis, University of Stavanger, Norway

[2] The Association for Materials Protection and Performance (2024) *Uniform Corrosion* https://www.ampp.org/technical-research/impact/corrosion-basics/group-1/uniform-corrosion

[3] The Association for Materials Protection and Performance (2024) *Pitting Corrosion* https://www.ampp.org/technical-research/impact/corrosion-basics/group-1/pitting-corrosion

[4] The Association for Materials Protection and Performance (2024) *Crevice Corrosion* https://www.ampp.org/technical-research/impact/corrosion-basics/group-1/crevice-corrosion

[5] The Association for Materials Protection and Performance (2024) *Galvanic Corrosion* https://www.ampp.org/technical-research/impact/corrosion-basics/group-1/galvanic-corrosion

[6] J. M. Kulicki and National Research Council (U.S.), Red. (1990) *Guidelines for evaluating corrosion effects in existing steel bridges*. i Report / National Cooperative Highway Research Program, no. 333. Washington, D.C: Transportation Research Board, National Research Council

[7] Industrial Inspection & Analysis (2021) *The Financial Cost of Rust and Corrosion*, The Risk of Rust https://industrial-ia.com/the-financial-cost-of-rust-and-corrosion/

[8] NS Trahair, MA Bradford, DA Nethercot and L Gardner (2008) *The behaviour and design of steel structures to EC3*, Taylor & Francis Group

[9] Demo Lab (2020) *Lateral Torsional Buckling - Shapes Comparison* https://www.youtube.com/watch?app=desktop&v=xEaYQBzU43g

[10] AF Hughes, DC Iles and AS Malik (2011) *Design of steel beams in torsion*, The Steel Construction Institute

[11] C.-K. Chiu, I.-H. Liao, E. Yamaguchi, and Y.-C. Lee (2023) *Journal of Constructional Steel Research: Study on the simplified evaluation method of the remaining load-carrying capacity of a corroded steel I-girder end using FEA*, Elsevier https://www.sciencedirect.com/science/article/pii/S0143974X23002729

[12] A. Bao, M. Gulasey, C. Guillaume, N. Levitova, A. Moraes, og C. Satter (2018) *Structural Capacity Analysis of Corroded Steel Girder Bridges* Presented at: International Conference on Civil, Strucutral and Transportation Engineering https://avestia.com/ICCSTE2018_Proceedings/files/paper/ICCSTE_118.pdf

[13] G. Tzortzinis, B. T. Knickle, A. Bardow, S. F. Breña, and S. Gerasimidis (2021) *Thin-Walled Structures: Strength evaluation of deteriorated girder ends. II: Numerical study on corroded I-beams*, Elsevier https://www.sciencedirect.com/science/article/pii/S0263823120310880

[14] NS EN 1993-2:2006+NA:2009 *Eurocode 3: Design of steel structures: Part 2: Steel Bridges*,

European Committee for Standardization

[15]G. Sedlacek (1991) *Traffic loads on road bridges* European development of EN 1991 - Eurocode 1 - Part 2

[16]S. C. Siriwardane (2021) *Chapter 3: Flexural members (Bending members)*

[17]Steelconstruction.info (2024) *3.2.6 Warping constant and torsional constant* https://industrial-ia.com/the-financial-cost-of-rust-and-corrosion/ co.uk)

[18]N. D. Adasooriya and S. C. Siriwardane (2014) *Remaining fatigue life estimation of corroded bridge members*, Fatigue & Fracture of Engineering Materials & Science (FFEMS) https://onlinelibrary.wiley.com/doi/10.1111/ffe.12144

[19]M. T. Gebremeskel, A. T. Cruz, and N. D. Adasooriya, (2023) *An approach for fatigue life assessment of a road bridge based on measured corrosion and actual traffic loading*, University of Stavanger; Faculty of Science and Technology, Norway

[20]Norgeskart (2024) *Norway; Hjelmeland; Ryfylkevegen; Storabru, Number; 970426* [ca. 1:75000], https://www.norgeskart.no/#!?project=norgeskart&layers=1002&zoom=14&lat=6589574.09&lon=-2196.50&p=searchOptionsPanel&markerLat=6589574.0891342955&markerLon=-2196.496209506276&sok=Ryfylkevegen

[21]A. H. Vang (2017) *Økning i bæreevne for stålbjelkebruer med betongdekke uten samvirke* Norges tekninsk-naturvitenskapelige universitet: Institutt for konstruksjonsteknikk

[22]Y. Sharifi and J. K. Paik (2011) *Thin-Walled Structures: Ultimate strength reliability analysis of corroded steel-box girder bridge*s, Elsevier https://www.sciencedirect.com/science/article/pii/S0263823110001576

[23]A. Aeran, S. C. Siriwardane, O. Mikkelsen, and I. Langen (2017) *Marine Structures: A framework to assess structural integrity of ageing offshore jacket structures for life extension*, Elsevier https://www.sciencedirect.com/science/article/pii/S0951833916303392?via%3Dihub

Appendix A:

In this appendix is the "Statens Vegvesen" reports of the bridge. This includes pictures of the bridge and the status report of the bridge.

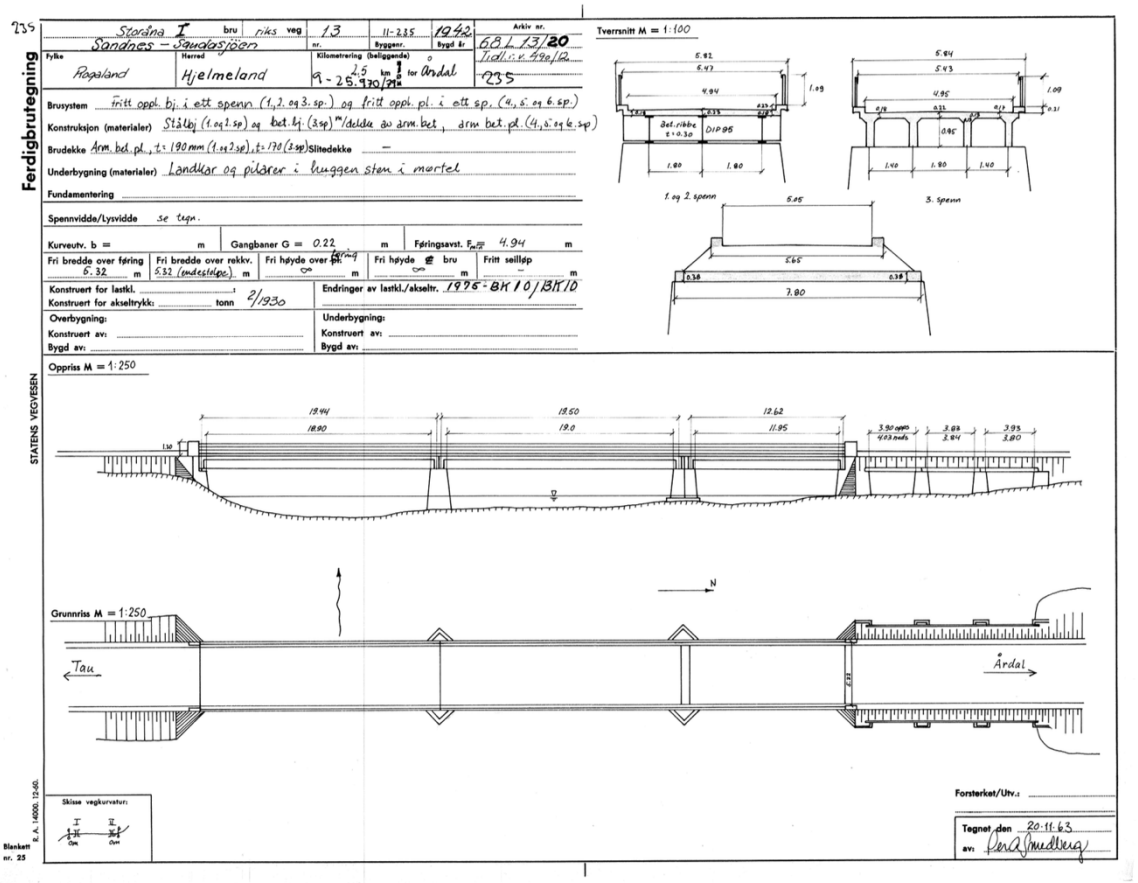

Figure: A.1

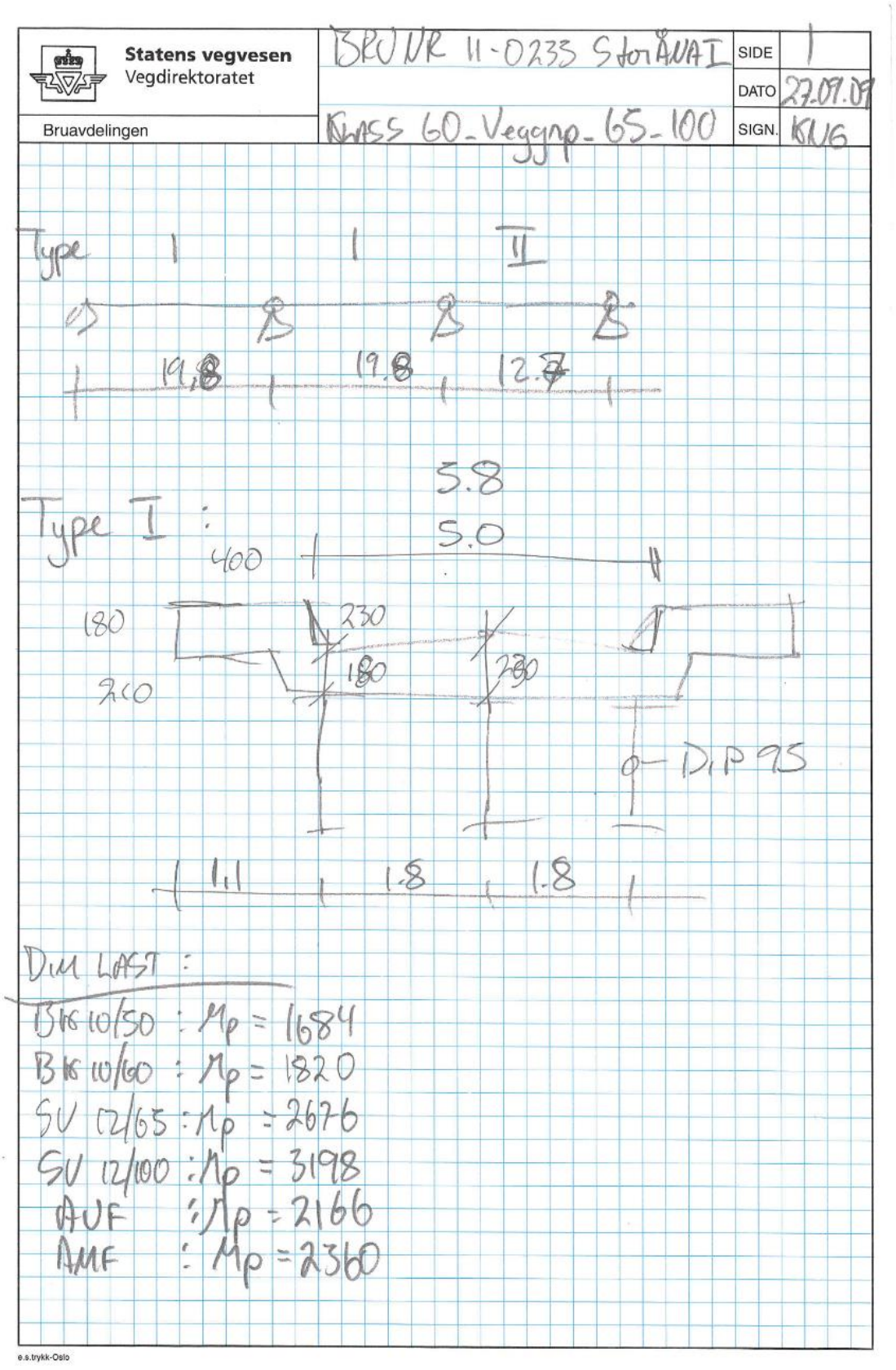
Statens vegvesen
Vegdirektoratet
Bruavdelingen
BRUNR 11-0233 Storåna I
Klasse 60_Veggrp_65_100
SIDE 1
DATO 27.09.07
SIGN. KUG
Type I I II
19.8
19.8
12.7
5.8
5.0
Type I :
400
180
210
230
180
230
DIP 95
1.1
1.8
1.8
DIM LAST :
TBK 10/50 : Mp = 1684
BK 10/60 : Mp = 1820
SV 12/65 : Mp = 2676
SV 12/100 : Mp = 3198
AUF : Mp = 2166
AMF : Mp = 2360
e.s.trykk-Oslo

Figure: A.2

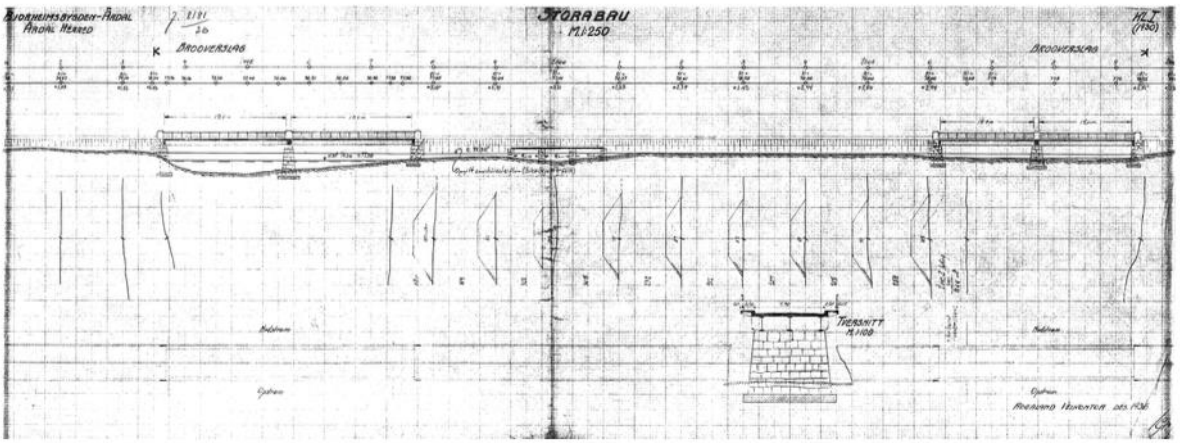

Figure: A.3

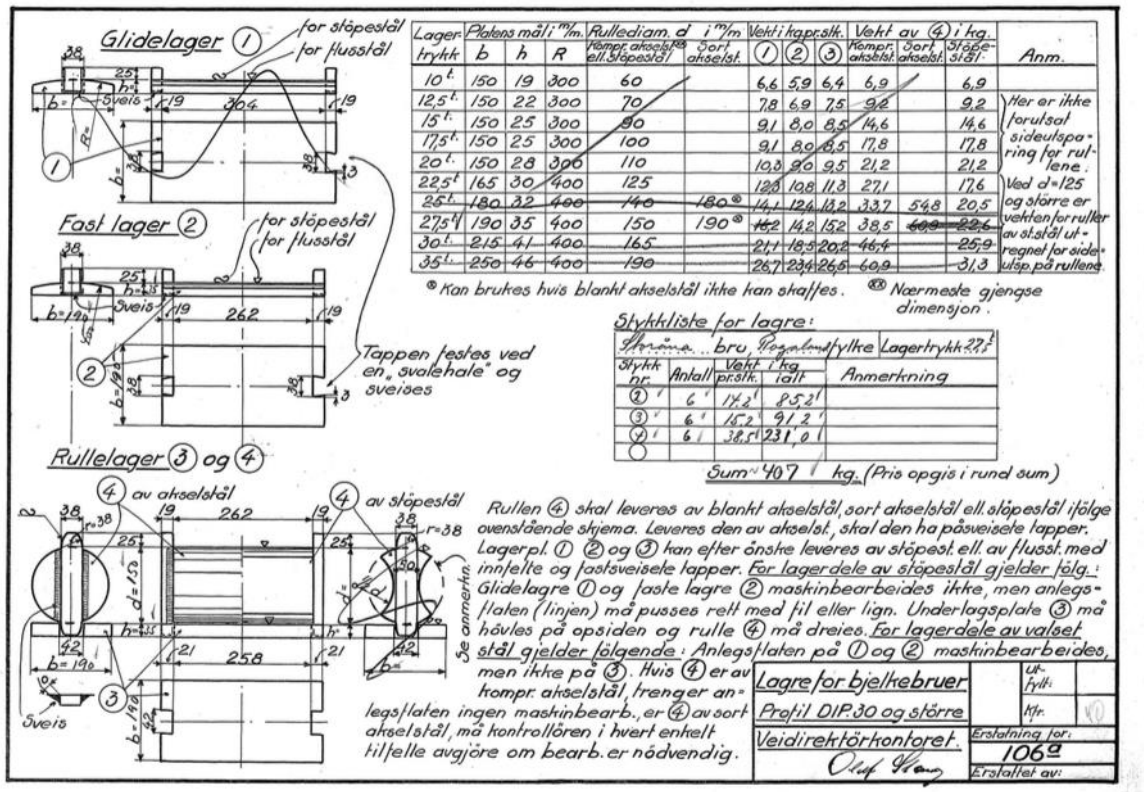

Figure: A.4

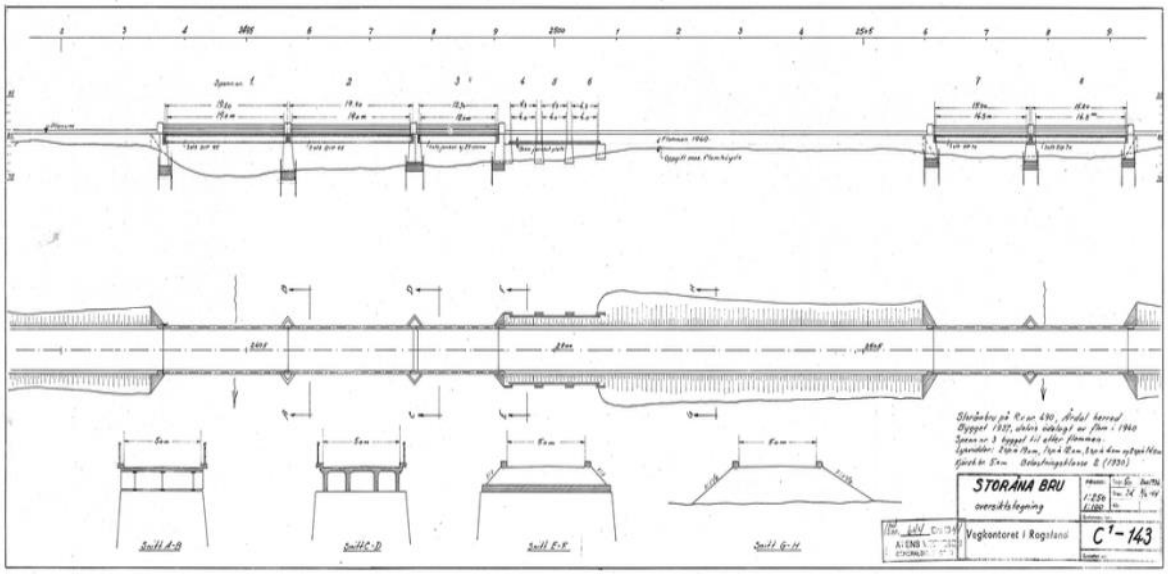

Figure: A.5

Figure: A.6

Figure: A.7

Figure: A.8

Figure: A.9

Byggverk	Vegreferanse	Kategori / type	Lengde / Antall spenn	Start akse	Slutt akse	Bru over
11-0235 Storåna I	P/RV13 S6D1 m7519	Vegbru / Stålbjelkebru	70.0 / 6	1-Mot Tau	7-Mot Årdal	Elv/Innsjø

Inspeksjonsrapport

Byggverksmerknad
Bygd i 1937, delvis ødelagt av flom i 1940. Bygd opp igjen og utvidet til som i dag i 1942. Bør renskes under (vannmeisling e.l.) og sprøytet på tørrbetong I spenn 1 og 2 er det benyttet DIP 95,dekke t=19cm.Dekke spenn 3 t=17cm.Dekke spenn 4,5 og 6 t=38cm. Nytt rekkverk ble satt opp vinter 2012 Bruarkiv vegdir.: JA Originaltegning vegdir.: E3

Tiltak

Tiltakstype	Beskrivelse	Årsak	Oppdragsansvarlig	Utførelsesdato	Intervall	Status	Kostnad	Merknad
Vedlikehold	Fjern vegetasjon pilarer			11.07.2021		Planlagt		
Vedlikehold	Renske betong og armering, samt mørtling. Gjelder hovedbjelke i betong og brudekke.			11.07.2021		Planlagt		
Vedlikehold	Rense og påføre nytt malesystem på hovedbjelker av stål			11.07.2021		Planlagt		

Inspeksjonsplan

Inspeksjonstype	Sist utført	Intervall	Planlagt utført	Tilkomst
Enkel inspeksjon	03.05.2021	1	03.05.2022	Ikke behov
Hovedinspeksjon	11.07.2018	5	11.07.2023	Ikke behov
Hovedinspeksjon u/vann	07.12.2018			Annet

Inspeksjonsdata

Utførelsesansvarlig	Utførelsesdato

Inspeksjonsmerknad
Ingen merknad er angitt

11-0235 Storåna I Side 1 av 11 Rapport hentet ut: 08.03.2022

Figure: A.10

Appendix B:

Appendix B includes the Python code which estimates the corrosion growth, and then plots the graphs for the different environments.

```
"""
Created on Wed Apr 17 16:24:19 2024

@author: ravnengamo
"""

import numpy as np
import matplotlib.pyplot as plt

# Constants
t = 120  # Constant t

# Function to calculate C(t) for given A, B, and t_0
def calculate_C(A, B, t_0):
    if t_0 >= t:
        print("Error: t_0 must be less than t.")
        return None
    return A * (t - t_0) ** B

# Input for t_0
t_0 = float(input("Enter the value of t_0: "))

# Constants for rural, urban, and marine lines
constants = {
    "rural": {"A": 0.034, "B": 1.0675745, "color": "green"},
    #"urban": {"A": 0.0802, "B": 0.593, "color": "red"},
    "marine": {"A": 0.0706, "B": 0.903964, "color": "blue"}
}

# Calculate C(t) for rural, urban, and marine lines
C_values = {}
for key, params in constants.items():
    A = params["A"]
    B = params["B"]
    color = params["color"]
    C_values[key] = calculate_C(A, B, t_0)
    print(f"{key.capitalize()} C(t) =", C_values[key])

# Plotting
t_values = np.linspace(t_0, t, 100)
plt.figure(figsize=(10, 6))
for key, params in constants.items():
    A = params["A"]
    B = params["B"]
    color = params["color"]
    C_values[key] = calculate_C(A, B, t_0)
    plt.plot(t_values, A * (t_values - t_0) ** B, label=f'{key.capitalize()} (C(t) = {A}(t - {t_0})^{B})', color=color)

plt.xlabel('t')
plt.ylabel('C(t)')
plt.title('Plot of C(t)')
plt.legend()
plt.grid(True)
plt.show()
```

Figure: B.1

Appendix C*:*

SAP2000: M_{cr}, $M_{b,Rd}$ and I_w is not considered when retrieving the data from SAP2000, as their values needed to be calculated manually.

4mm corroded:

Units : KN, mm, C

Units KN, mm, C

Frame : 1 X Mid: 0, Combo: Live only Design Type: Beam
Length: 19000, Y Mid: 0, Shape: dip korr Frame Type: DCH-MRF
Loc : 19000, Z Mid: 0, Class: Class 3 Rolled : No

Country=CEN Default Combination=Eq. 6.10 Reliability=Class 2
Interaction=Method 2 (Annex B) MultiResponse=Envelopes P-Delta Done? No
Consider Torsion? No

GammaM0=1, GammaM1=1, GammaM2=1,25
An/Ag=1, RLLF=1, PLLF=0,75 D/C Lim=0,95

Aeff=37980,269 eNy=0, eNz=0,
A=37980,269 Iyy=6479123275, iyy=379,819 Wel,yy=11302665,75 Weff,yy=11302665,7
It=12652020,26 Izz=143673696,2 izz=61,505 Wel,zz=955807,183 Weff,zz=955807,183
Iw=0, Iyz=0, h=950, Wpl,yy=13342886,75 Av,y=20951,117
E=210, fy=0,275 fu=0,43 Wpl,zz=1559628,167 Av,z=10017,166

STRESS CHECK FORCES & MOMENTS

Location	Ned	Med,yy	Med,zz	Ved,z	Ved,y	Ted
19000,	0,	0,	0,116	0,01	0,	0,

PMM DEMAND/CAPACITY RATIO (Governing Equation EC3 6.3.3(4)-6.62)
D/C Ratio: 0, = 0, + 0, + 0, < 0,95 OK
= NEd/(Chi_z NRk/GammaM1) + kzy (My,Ed+NEd eNy)/(Chi_LT My,Rk/GammaM1)
+ kzz (Mz,Ed+NEd eNz)/(Mz,Rk/GammaM1) (EC3 6.3.3(4)-6.62)

AXIAL FORCE DESIGN

	Ned Force	Nc,Rd Capacity	Nt,Rd Capacity
Axial	0,	10444,574	10444,574

Npl,Rd	Nu,Rd	Ncr,T	Ncr,TF	An/Ag
10444,574	11758,651	6848,023	759,567	1,

	Curve	Alpha	Ncr	LambdaBar	Phi	Chi	Nb,Rd
Major (y-y)	c	0,49	28966,747	0,6	0,778	0,795	8200,062
MajorB(y-y)	c	0,49	28966,747	0,6	0,778	0,795	8200,062
Minor (z-z)	c	0,49	759,567	3,708	8,235	0,064	670,059
MinorB(z-z)	c	0,49	759,567	3,708	8,235	0,064	670,059
Torsional TF	c	0,49	759,567	3,708	8,235	0,064	670,059

MOMENT DESIGN

	Med Moment	Med,span Moment	Mc,Rd Capacity	My,Rd Capacity	Mn,Rd Capacity	Mb,Rd Capacity
Major (y-y)	0,	49,005	3108233,082	3108233,082	3108233,082	672412,859
Minor (z-z)	0,	0,116	262846,975	262846,975	262846,975	

	Curve	AlphaLT	LambdaBarLT	PhiLT	ChiLT	Iw	Mcr
LTB	d	0,76	1,763	2,647	0,216	0,	1000388,817

	kw	C1	C2	C3		
Factors	1,	1,132	0,459	0,525		
	za	zs	zg	zm	zj	
	-9,717	0,	-9,717	-7,008	7,008	

	kyy	kyz	kzy	kzz
Factors	0,95	1,	1,	1,

	Ved Force	Vpl.Rd Capacity	Ved/Vpl.Rd Ratio	rho Factor
Major (z)	0,01	2860,608	3,461E-06	1,
Minor (y)	0,	3326,435	0,	1,

SHEAR DESIGN

	Ved Force	Ted Torsion	Vc,Rd Capacity	Stress Ratio	Status Check
Major (z)	0,01	0,	2860,608	3,461E-06	OK
Minor (y)	0,	0,	3326,435	0,	OK

	Vpl,Rd Capacity	Eta Factor	Lambdabar Ratio	Chi Factor
Minor (y)	2860,608	1,2	0,	1,
Major (y)	3326,435	1,2	0,	1,

Figure: C.1

4.3655mm corroded

Units : KN, mm, C — Units: KN, mm, C

Frame : 1	X Mid: 0,	Combo: Live only	Design Type: Beam		
Length: 19800,	Y Mid: 0,	Shape: 4.5366 ny	Frame Type: DCH-MRF		
Loc : 19800,	Z Mid: 0,	Class: Class 3	Rolled : No		
Country=CEN Default		Combination=Eq. 6.10		Reliability=Class 2	
Interaction=Method 2 (Annex B)		MultiResponse=Envelopes		P-Delta Done? No	
Consider Torsion? No					
GammaM0=1,	GammaM1=1,	GammaM2=1,25			
An/Ag=1,	RLLF=1,	PLLF=0,75	D/C Lim=0,95		
Aeff=3,764E+10	eNy=0,	eNz=0,			
A=3,764E+10	Iyy=6,409E+21	iyy=379097,660	Wel,yy=1,113E+16	Weff,yy=1,113E+16	
It=1,209E+19	Izz=1,411E+20	izz=61225,325	Wel,zz=9,375E+14	Weff,zz=9,379E+14	
Iw=0,	Iyz=0,	h=950000,	Wpl,yy=1,319E+16	Av,y=2,061E+10	
E=210,	fy=0,275	fu=0,43	Wpl,zz=1,536E+15	Av,z=1,799E+10	

STRESS CHECK FORCES & MOMENTS

Location	Ned	Med,yy	Med,zz	Ved,z	Ved,y	Ted
19800,	0,	0,	0,133	0,01	0,	0,

EN1993-1-1 DEMAND/CAPACITY RATIO (Governing Equation EC3 6.3.3(4)-6.62)

D/C Ratio: 0, = 0, + 0, + 0, < 0,95 OK

= NEd/(Chi_z NRk/GammaM1) + kzy (My,Ed+NEd eNy)/(Chi_LT My,Rk/GammaM1) + kzz (Mz,Ed+NEd eNz)/(Mz,Rk/GammaM1) (EC3 6.3.3(4)-6.62)

AXIAL FORCE DESIGN

	Ned Force	Nc,Rd Capacity	Nt,Rd Capacity
Axial	0,	1,035E+10	1,035E+10

Npl,Rd	Nu,Rd	Ncr,T	Ncr,TF	An/Ag
1,035E+10	1,165E+10	6622768169,	6622768169,	1,

	Curve	Alpha	Ncr	LambdaBar	Phi	Chi	Nb,Rd
Major (y-y)	c	0,49	2,859E+16	6,016E-04	0,451	1,	1,035E+10
MajorB(y-y)	c	0,49	2,859E+16	6,016E-04	0,451	1,	1,035E+10
Minor (z-z)	c	0,49	7,458E+14	0,004	0,452	1,	1,035E+10
MinorB(z-z)	c	0,49	7,458E+14	0,004	0,452	1,	1,035E+10
Torsional TF	c	0,49	6622768169,	1,25	1,539	0,411	4249170401,

MOMENT DESIGN

	Med Moment	Med,span Moment	Mc,Rd Capacity	Mv,Rd Capacity	Mn,Rd Capacity	Mb,Rd Capacity
Major (y-y)	0,	49,005	3,060E+15	3,060E+15	3,060E+15	3,060E+15
Minor (z-z)	0,	0,133	2,579E+14	2,579E+14	2,579E+14	

	Curve	AlphaLT	LambdaBarLT	PhiLT	ChiLT	Iw	Mcr
LTB	d	0,76	0,014	0,429	1,	0,	1,572E+19

Factors	kw	C1	C2	C3		
	1,	1,132	0,459	0,525		
	za	zs	zg	zz	zj	
	-11091,308	0,	-11091,308	-7970,988	7970,988	

	kyy	kyz	kzy	kzz
Factors	0,95	1,	1,	1,

	Ved Force	Vpl.Rd Capacity	Ved/Vpl.Rd Ratio	rho Factor
Major (z)	0,01	2856880268,	0,	1,
Minor (y)	0,	3272802680,	0,	1,

SHEAR DESIGN

	Ved Force	Ted Torsion	Vc,Rd Capacity	Stress Ratio	Status Check
Major (z)	0,01	0,	2856880268,	0,	OK
Minor (y)	0,	0,	3272802680,	0,	OK

	Vpl,Rd Capacity	Eta Factor	Lambdabar Ratio	Chi Factor
Minor (y)	2856880268,	1,2	0,	1,
Major (y)	3272802680,	1,2	0,	1,

Figure: C.2

5.349mm corroded

Units : KN, mm, C

Units KN, mm, C

Frame : 1 X Mid: 0, Combo: Live only Design Type: Beam
Length: 19800, Y Mid: 0, Shape: 5.349 ny Frame Type: DCH-MRF
Loc : 19800, Z Mid: 0, Class: Class 3 Rolled : No

Country=CEN Default Combination=Eq. 6.10 Reliability=Class 2
Interaction=Method 2 (Annex B) MultiResponse=Envelopes P-Delta Done? No
Consider Torsion? No

GammaM0=1, GammaM1=1, GammaM2=1,25
An/Ag=1, RLLF=1, PLLF=0,75 D/C Lim=0,95

Aeff=3,721E+10	eNy=0,	eNz=0,		
A=3,721E+10	Iyy=5,319E+21	iyy=378094,081	Wel,yy=1,090E+16	Weff,yy=1,090E+16
It=1,166E+15	Izz=1,372E+20	izz=60730,263	Wel,zz=9,119E+14	Weff,zz=9,119E+14
Iw=0,	Iyz=0,	h=950000,	Wpl,yy=1,299E+16	Av,y=2,019E+10
E=210,	fy=0,275	fu=0,43	Wpl,zz=1,502E+15	Av,z=1,797E+10

STRESS CHECK FORCES & MOMENTS

Location	Ned	Med,yy	Med,zz	Ved,z	Ved,y	Ted
19800,	0,	0,	0,161	0,01	0,	0,

PMM DEMAND/CAPACITY RATIO (Governing Equation EC3 6.3.3(4)-6.62)
D/C Ratio: 0, + 0, + 0, < 0,95 OK
= NEd/(Chi_z NRk/GammaM1) + kzy (My,Ed+NEd eNy)/(Chi_LT My,Rk/GammaM1)
+ kzz (Mz,Ed+NEd eNz)/(Mz,Rk/GammaM1) (EC3 6.3.3(4)-6.62)

AXIAL FORCE DESIGN

	Ned Force	Nc,Rd Capacity	Nt,Rd Capacity
Axial	0,	1,023E+10	1,023E+10

Npl,Rd	Nu,Rd	Ncr,T	Ncr,TF	An/Ag
1,023E+10	1,152E+10	6420492859,	6420492859,	1,

	Curve	Alpha	Ncr	LambdaBar	Phi	Chi	Nb,Rd
Major (y-y)	c	0,49	2,812E+16	6,032E-04	0,451	1,	1,023E+10
MajorB(y-y)	c	0,49	2,812E+16	6,032E-04	0,451	1,	1,023E+10
Minor (z-z)	c	0,49	7,255E+14	0,004	0,452	1,	1,023E+10
MinorB(z-z)	c	0,49	7,255E+14	0,004	0,452	1,	1,023E+10
Torsional TF	c	0,49	6420492859,	1,262	1,557	0,405	4144823836,

MOMENT DESIGN

	Med Moment	Med,span Moment	Mc,Rd Capacity	Mv,Rd Capacity	Mn,Rd Capacity	Mb,Rd Capacity
Major (y-y)	0,	49,005	2,996E+15	2,996E+15	2,996E+15	2,996E+15
Minor (z-z)	0,	0,161	2,508E+14	2,508E+14	2,508E+14	

	Curve	AlphaLT	LambdaBarLT	PhiLT	ChiLT	Iw	Mcr
LTB	d	0,76	0,013	0,429	1,	0,	1,810E+19

Factors	kw	C1	C2	C3
	1,	1,132	0,459	0,525

za	zs	zg	zz	zj
-13169,404	0,	-13169,404	-9420,229	9420,229

	kyy	kyz	kzy	kzz
Factors	0,95	1,	1,	1,

	Ved Force	Vpl,Rd Capacity	Ved/Vpl,Rd Ratio	rho Factor
Major (z)	0,01	2853826017,	0,	1,
Minor (y)	0,	3206083920,	0,	1,

SHEAR DESIGN

	Ved Force	Ted Torsion	Vc,Rd Capacity	Stress Ratio	Status Check
Major (z)	0,01	0,	2853826017,	0,	OK
Minor (y)	0,	0,	3206083920,	0,	OK

	Vpl,Rd Capacity	Eta Factor	Lambdabar Ratio	Chi Factor
Minor (y)	2853826017,	1,2	0,	1,
Major (y)	3206083920,	1,2	0,	1,

Figure: C.3

Appendix D:

Appendix D includes the Excel formula sheet for calculations. Including one file with formulas only and one with numbers.

(A) simplified method: DIP 95			Lambda F:		Dimensions:		Torsional calculations It:		Area calculations:		Ekstra dimensions:	
fy=	275		kc=	0,93	H=	950	D1=	52,2526042	A symetric=	39054,5666	tf,topp=	32
E=	210000		Lc=	19800	B=	300	ALPHA 1=	0,12900008			tf,bottom=	28
Lambda f=	2,745386883		ifz=	77,2700882	tf=	36			A unsymetric=	35202,5666	tf,half topp Le	32
kf=	1,1		strain=	0,92441628	tw=	19					tf,half topp Ri	36
Alpha=	0,76	Curve d	lambda 1=	86,8026885	r=	30			A corroded=	34178,8584	tf,half bottom	28
Sy=	6943344,215				HZZ=	914					tf,half bottom	36
Phi=	5,235821585		Lambda f=	2,74538688	IFZ=	81083641,69						
shi x=	0,103155012				AFZ=	13580,33333						
Gama o=	1,05										Bf,topp=	292
G=	81000										Bf,bottom=	292
Mb,rd=	412,6911019	KNM										
Mc,Rd=	3636,989827	KNM										
(B) Conservative method: DIP 95					M critical Calculations:							
Lambda LT=	1,891225599				Iz=	143673696,2		162752308	Andre program			
shi LT=	0,193413193				Iw=	3,00061E+13		3,399E+13	Andre program			
Phi LT=	2,93103286				It=	12552020		11420908,7	Andre program			
					Alpha M=	1,13						
Mb,rd=	703,4418145				Mzx=	944857395,2						
Mc,Rd=	3636,989827				Mcr=	[redacted]	Nmm	Should be Nmm				
					MCR=	1067688857						
					LAMBDA LT	1,891225599						
					PHI LT	2,93103286						
					SHI LT	0,193413193						
					MB;RD=	703,4418145	KNM					

Figure: D.1

(A) simplified method: DIP			Lambda F:		Dimensions:		Torsional calculations It:		
fy=	275		kc=	0,93	H=	950	D1=	=((J5+I7)^2+(I7+0,25*I6)*I6)/(2*I7+I5)	
E=	210000		Lc=	19800	B=	300	ALPHA 1=	=-0,042+0,2204*(I6/I5)+0,1355*(I7/I5)-0,0865*(I7*I6/I5^2)-0,0725*(I6^2/I5^2)	
Lambda f=	=F9		ifz=	=ROT(I9/I10)	tf=	36			
kf=	1,1		strain=	=ROT(235/B3)	tw=	19			
Alpha=	0,76	Curve d	lambda 1=	=93,9*F6	r=	30			
Sy=	=13886688,43/2				HZZ=	=I3-I5			
Phi=	=0,5*(1+B7*(B5-0,2)+B5^2)		Lambda f=	=(F3*F4)/(F5*F7)	IFZ=	=(1/12*I5*I4^3)+(1/12*((I3-2*I5)/6)*I6^3)			
shi x=	=1/(B9+ROT(B9^2-B5^2))				AFZ=	=I4*I5+((I3-2*I5)/6)*I6			
Gama o=	=1,05								
G=	81000								
Mb,rd=	=B6*B10*B14	KNM							
Mc,Rd=	=2*B8*B3/B11/1000000	KNM							
(B) Conservative method: I					M critical Calculations:				
Lambda LT=	=ROT((2*B8*B3)/J26)				Iz=	143673696,2		162752308	Andre program
shi LT=	=1/(B21+ROT(B21^2-B19^2))				Iw=	=(J19*J8^2)/4		33990000000000	Andre program
Phi LT=	=0,5*(1+B7*(B19-0,2)+B19^2)				It=	12552020		11420908,67	Andre program
					Alpha M=	1,13			
Mb,rd=	=(B20*2*B8*B3)/B11/1000000				Mzx=	=PI()/F4*ROT(B4*J19*B12*J21)*ROT(1+((PI()/F4)^2*(B4*J20/B12/J21)))			
Mc,Rd=	=2*B8*B3/B11/1000000				Mcr=	[redacted]	Nmm	Should be Nmm	
					MCR=	=J25*J22			
					LAMBDA LT	=ROT(2*B8*B3/J28)			
					PHI LT	=0,5*(1+B7*(J30-0,2)+J30^2)			
					SHI LT	=1/(J32+ROT(J32^2-J30^2))			
					MB;RD=	=B26*J34	KNM		

Figure: C.2